NASA TECHNICAL NOTE

NASA TN D-5385

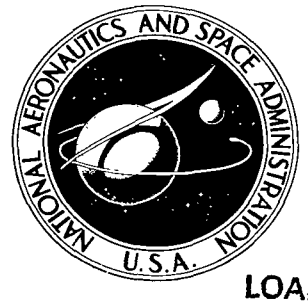

NASA TN D-5385

ANALYSIS OF TOTAL-PRESSURE LOSS AND AIRFLOW DISTRIBUTION FOR ANNULAR GAS TURBINE COMBUSTORS

by Robert R. Tacina and Jack Grobman

Lewis Research Center
Cleveland, Ohio

NATIONAL AERONAUTICS AND SPACE ADMINISTRATION • WASHINGTON, D. C. • AUGUST 1969

ANALYSIS OF TOTAL-PRESSURE LOSS AND AIRFLOW DISTRIBUTION FOR ANNULAR GAS TURBINE COMBUSTORS

By Robert R. Tacina and Jack Grobman

Lewis Research Center
Cleveland, Ohio

NATIONAL AERONAUTICS AND SPACE ADMINISTRATION

For sale by the Clearinghouse for Federal Scientific and Technical Information
Springfield, Virginia 22151 – CFSTI price $3.00

ABSTRACT

Using a previously developed computer program for the analysis of the annular gas turbine combustor, the effects of a number of geometric and flow variables on the total pressure loss and airflow distribution were calculated. The results, where comparable, agree very well with previously calculated tubular combustor data. The following are significant extensions to the previously available data: (1) an increased range of open hole area in the dome, (2) combined effect of reference Mach number and heat release, (3) the use of a liner hole with a scoop, (4) the use of a liner in which the cross-sectional area varies with length.

ANALYSIS OF TOTAL-PRESSURE LOSS AND AIRFLOW DISTRIBUTION FOR ANNULAR GAS TURBINE COMBUSTORS

by Robert R. Tacina and Jack Grobman

Lewis Research Center

SUMMARY

A previously developed computer program permits the calculation of flow conditions along the liner and annulus of gas turbine combustors. It does this by solving the equations of momentum, energy, continuity, and state. In this report the effect of a number of geometric and flow variables on the total pressure loss and airflow distribution were calculated using the computer program. The combustor total pressure loss coefficient and liner airflow distribution are presented graphically in terms of the following dimensionless parameters: (1) ratio of hole area in liner to reference cross-sectional area, (2) ratio of the liner cross-sectional area to reference cross-sectional area, (3) ratio of hole area in combustor dome to hole area in liner, (4) combustor reference Mach number, and (5) ratio of combustor exit to inlet total temperature. The results that were compared agreed well with previously calculated tubular combustor data.

The following are significant extensions to the previously available data: (1) an increased range of open hole area in the dome, (2) combined effect of reference Mach number and heat release, (3) the use of a liner hole with a scoop, (4) the use of a liner in which the cross-sectional area varies with length.

Other variables that were studied include liner length, the number of hole rows, axial hole distribution, ratio of liner open area on outer liner wall to total liner open area, combustor outer diameter, and the dilution jet mixing model.

INTRODUCTION

A computer program for the analysis of annular gas turbine combustors was developed and reported in references 1 and 2. This computer program can calculate the efficiency of the diffuser, the static and total pressures along the length of the combustor, the airflow distribution, and flame and wall temperatures of the combustor. The purpose

of this report is to use the computer program to obtain the total pressure loss and fractional liner airflow distribution for annular combustors and where comparison is valid compare this data with the tubular combustor data from reference 3.

Generalized curves are presented from which preliminary estimates of the total pressure loss and airflow distribution can be made from the combustor geometry and operating conditions. These calculations do not include the diffuser pressure loss. These curves are similar to those found in reference 3, with the exception that the range of some of the variables has been extended while other variables have been added.

The total pressure loss coefficient and fractional liner airflow distribution are obtained as functions of the following dimensionless parameters: (1) ratio of hole area in liner to reference cross-sectional area, (2) ratio of the liner cross-sectional area to reference cross-sectional area, (3) ratio of open hole area in dome to open area in liner, (4) combustor reference Mach number, and (5) ratio of combustor-exit to inlet total temperature.

Other variables studied for their effect on the total pressure loss coefficient and fractional liner airflow distribution were: liner air entry geometry, liner length, the number of hole rows, axial hole distribution, hole proportion on inner and outer liner wall, varying liner cross-sectional area along the combustor length, film cooling slot area, and the combustor diameter. In addition the effects of various calculation options available in the computer program were studied.

METHOD OF ANALYSIS

The overall total pressure loss in the gas turbine combustor results mainly from: (1) losses in the diffuser, (2) losses in the mixing of the dilution jets with the liner gas stream, (3) losses from heat addition, (4) losses due to wall friction, and (5) losses in diffusion of annulus air. Only the latter four sources of pressure loss are considered herein. Data on diffuser losses for annular combustors can be found in references such as reference 4.

The results to be presented pertain to a typical annular gas turbine combustor such as shown schematically in figure 1. The effects of the inlet diffuser and combustor snout are ignored. The inlet airflow is split between flow entering the liner through holes in the inner and outer annuli and flow entering the liner through openings in the combustor dome.

The total pressure loss is defined as the reduction in total pressure from station 3 to station 4 neglecting any effect of the diffuser. The combustor total pressure loss coefficient is defined as the ratio of this total pressure loss to the reference dynamic pressure, $\Delta P/q_{ref}$. The symbols are defined in appendix A. The total pressure loss is obtained from a solution of the equations of momentum, energy, continuity, and state for

each air entry port along the length of the combustor. Data are also obtained on the liner airflow distribution, and the static and total pressures in the annuli and liner along the length of the combustor.

The data were obtained for assigned values of combustor geometry and operating conditions by using the computer program developed in references 1 and 2.

The major assumptions made in the development of the computer program were that the flow is steady-state and one-dimensional and that the primary zone is a stirred reactor. A discussion of the assumptions and the methods of calculation is presented in appendix B. A detailed description of the computer program is given in references 1 and 2.

SCOPE OF CALCULATIONS

Combustor Geometry

Combustor total pressure loss and airflow distribution were obtained as a function of the following dimensionless geometric variables:

(1) Ratio of open area in liner to reference area, $A_{H,liner}/A_{ref}$

(2) Ratio of cross-sectional area of liner to reference area, A_L/A_{ref}

(3) Ratio of open area in dome to open area in liner, $A_{H,dome}/A_{H,liner}$

These calculations were performed for a representative combustor geometry (fig. 1) with the following design assumptions:

(1) The outer casing diameter is 40 inches (1.016 m) and the inner casing diameter is 20 inches (0.508 m) along the entire length of the combustor.

(2) The combustor liner is 20 inches (0.508 m) long.

(3) Liner cross-sectional area is constant along the length of the combustor.

(4) The inner and outer annulus areas are constant and equal along the length of the combustor.

(5) The air entry ports in the liner consist of 3/4-inch (0.019-m) diameter flush holes.

(6) The air entry areas of each hole row are equal and the rows are spaced equally.

(7) There are equal air entry areas on the inner and outer liner wall.

(8) There are 19 hole rows along the axis of the combustor.

(9) All airflow enters the combustor liner (zero bypass cooling air at combustor exit).

In addition, calculations were performed to study the independent influence on the following geometric variables on the results for the representative combustor geometry:

(1) Liner air-entry-port configuration

(2) Liner length

(3) Number of hole rows

(4) Axial hole distribution

(5) Proportion of air entry ports on inner and outer liner wall

(6) Varying liner cross-sectional area along the combustor length

(7) Combustor outer diameter

Combustor Flow Variables

The effect of the following flow variables on the total pressure loss coefficient and airflow distribution were obtained:

(1) Reference Mach number, M_{ref}

(2) Ratio of exit to inlet temperature, T_4/T_3

These calculations were performed on the previously described representative combustor geometry with the following flow assumptions:

(1) The combustor inlet velocity profile is flat.

(2) Combustor inlet total temperature is 600^{o} F (588 K).

(3) Combustor inlet total pressure is 150 psia (10 atm).

RESULTS AND DISCUSSION

Combustor Total Pressure Loss Coefficient

Effect of liner open hole area and liner cross-sectional area. - Figure 2 shows the variation of $\Delta P/q_{ref}$ with the ratio of liner open hole area to combustor reference area, $A_{H,liner}/A_{ref}$, for values of the ratio of the liner cross-sectional area to combustor reference area, A_L/A_{ref} of 0.5, 0.6, 0.7, and 0.85. Figure 2(a) shows that for any given value of A_L/A_{ref}, the total pressure loss coefficient, $\Delta P/q_{ref}$ asymptotically approaches a minimum value as $A_{H,liner}/A_{ref}$ increases over a value of about 1.0 and $\Delta P/q_{ref}$ increases rapidly as $A_{H,liner}/A_{ref}$ decreases to values below about 1.0.

Figure 3 shows the variation of $\Delta P/q_{ref}$ with A_L/A_{ref} for various values of ratio of open area in dome to open area in liner $A_{H,dome}/A_{H,liner}$. For any given value of $A_{H,dome}/A_{H,liner}$ the minimum value for the total pressure loss coefficient, $\Delta P/q_{ref}$ shifts to higher values of A_L/A_{ref} as the ratio of exit to inlet temperature T_4/T_3 increases. Figure 3 also shows that for a given value of T_4/T_3, the minimum value of $\Delta P/q_{ref}$ shifts to higher values of A_L/A_{ref} as $A_{H,dome}/A_{H,liner}$ is increased. This effect is more pronounced at higher values of T_4/T_3. Most of the trends described herein were also obtained in the analysis for the tubular combustor in reference 3.

In figures 2, 3, and many of the later figures in this report, the curves often end abruptly because the computer program had failed to converge. Failure of the program to converge for a given set of variables was attributed to a reversal of flow from the

liner to the annulus. The computer program is not capable of handling the case of reverse flow. No attempt was made to find the exact point where the program failed to converge for the following reasons: (1) the data that did converge covered what was felt to be the range of interest and (2) due to limitations in the program the exact point at which the program failes to converge is not very meaningful.

Effect of combustor total open hole area and open hole area in combustor dome. - The ratio of the combined open hole area in the combustion chamber to the combustor reference area $A_{H,total}/A_{ref}$ including the air entry ports in both the liner and dome may be expressed by $A_{H,liner}/A_{ref}\,(1 + A_{H,dome}/A_{H,liner})$. In figure 4 $\Delta P/q_{ref}$ is plotted against $A_{H,total}/A_{ref}$ for various values of $A_{H,dome}/A_{H,liner}$. For a fixed value of $A_{H,total}/A_{ref}$, the total pressure loss coefficient, $\Delta P/q_{ref}$ is reduced as $A_{H,dome}/A_{H,liner}$ is increased. This effect is partly explained by the fact that in the calculations, the discharge coefficients of air entry ports in the dome are always greater than those for flush air entry ports in the liner wall. As indicated in appendix B, the discharge coefficients of air entry ports in the dome were assumed to be 0.6, while the discharge coefficients of air entry ports in the liner varied over a range from about 0.1 at the front end of the liner to about 0.6 at the rear of the liner.

Effect of combustor reference Mach number. - The effect of reference Mach number, M_{ref} on the total pressure loss coefficient $\Delta P/q_{ref}$ is shown in figure 5. The increase in $\Delta P/q_{ref}$ with M_{ref} is shown to be more pronounced at the higher value of the combustor exit to inlet total temperature ratio, T_4/T_3. For a value of T_4/T_3 of 1.0, the increase in $\Delta P/q_{ref}$ is shown to be negligible for values of A_L/A_{ref} of 0.5 and 0.6 and is shown to be small for a value of A_L/A_{ref} of 0.7. For a value of T_4/T_3 of 3.0, the rate of increase of $\Delta P/q_{ref}$ with M_{ref} is shown to be significant for values of M_{ref} greater than about 0.08 especially at a value of A_L/A_{ref} of 0.5, and the rate of increase of $\Delta P/q_{ref}$ with M_{ref} is shown to be least for a value of A_L/A_{ref} of 0.7.

Effect of heat release. - Figure 6 shows the effect of heat release on the total pressure loss coefficient $\Delta P/q_{ref}$. $\Delta P/q_{ref}$ is plotted against the ratio of exit to inlet total temperature, T_4/T_3 for various ratios of liner cross-sectional area to reference area A_L/A_{ref}. The total pressure loss coefficient increases with T_4/T_3 at a more rapid rate as A_L/A_{ref} decreases. The dependence of the rate of increase of $\Delta P/q_{ref}$ with T_4/T_3 on A_L/A_{ref} is shown more clearly in figure 7. Figure 7 shows that the minimum value $\Delta P/q_{ref}$ for a given value of T_4/T_3 shifts to higher values of A_L/A_{ref} as the values of T_4/T_3 are increased. These effects are similar to those noted previously for the tubular combustor in reference 3.

Effect of liner air entry geometry. - The results presented in the previous sections of this report were computed using liner air entry port discharge coefficient data for a 3/4-inch (0.019-m) diameter hole obtained from reference 5. Reference 5 concluded that for circular holes, the effects of hole size, and wall thickness on discharge coefficient were small compared to the effect of a correlating flow parameter $(P_{an} - p_L)/(P_{an} - p_{an})$.

Other factors such as annulus height, boundary-layer thickness, and pressure level had a negligible effect on discharge coefficient. Similarly, reference 6 found that the effects of size or shape of flush rectangular holes on discharge coefficient were small. Consequently, the discharge coefficient data for the 3/4-inch (0.019-m) diameter hole used in these computations should be representative for all flush-air-entry ports in the liner. Reference 6 showed that the effect of adding a scoop to a flush hole was to extend the flow range to lower values of the correlating flow parameter $(P_{an} - p_L)/(P_{an} - p_{an})$ as seen in figure 8. In figure 8 the discharge coefficient, C_p, corrected to a static pressure ratio of unity is plotted against the correlating flow parameter $(P_{an} - p_L)/(P_{an} - p_{an})$. The ratio C_d/C_p is plotted against the static pressure ratio, p_{an}/p_L (P_{an}/p_L for the holes with scoops) in figure 9. The discharge coefficient is obtained from $C_d = C_p(C_d/C_p)$.

Figure 10 shows the variation of $\Delta P/q_{ref}$ with $A_{H,liner}/A_{ref}$ for two different liner air-entry geometries. Data for a typical scoop with a value of A_f/A_h of 1.378 is compared to the previously shown data for the flush hole. The scoop has the lower value of $\Delta P/q_{ref}$ as would be expected from the influence of the discharge coefficient data of figure 8 on the effective area of each air-entry geometry.

Effect of film cooling slots. - The results described in the previous sections were for combustors with air-entry ports for penetrating jets only. Since practical considerations for the cooling of the liner wall require the inclusion of some type of wall jet for film cooling, the effect on $\Delta P/q_{ref}$ of adding a typical film cooling slot to the combustor is shown in figure 11. The discharge coefficient data for the cooling slot geometry used in these computations shown in figure 8 was again obtained from reference 6 for a step louver with a height of 0.104 inch (0.0026 m). Reference 6 indicates that the effect of height is small for values of the correlating flow parameter above 1.0 and that the data used for a height of 0.104 inch (0.0026 m) should be fairly representative of practically sized continuous step louvers.

The cooling slots were assumed to be continuous step louvers with evenly proportioned area along the length of the combustor at values of thr fractional length x/L of 0.05, 0.25, 0.50, 0.75, and 0.95. The value for $A_{H,liner}$ includes the face area of the cooling slot. The observed decrease in $\Delta P/q_{ref}$ as $A_c/A_{H,liner}$ is increased is to be expected due to the higher values for the discharge coefficient of step louvers compared to flush holes.

Effect of liner length. - In the preceding results, the liner length was assumed to be 20 inches (0.508 m). The variation of $\Delta P/q_{ref}$ with liner length was investigated for values of A_L/A_{ref} of 0.6, $A_{H,liner}/A_{ref}$ of 0.8, $A_{H,dome}/A_{H,liner}$ of 0.1, M_{ref} of 0.094, and T_4/T_3 of 1.0 and 2.5. The values of $\Delta P/q_{ref}$ for liner lengths of 10, 20, and 40 inches (0.254, 0.508, and 1.016 m) are 6.86, 6.90, and 6.98, respectively, for exit to inlet total temperature ratio T_4/T_3 of 1.0, and 10.38, 10.42, and 10.50, respectively, for T_4/T_3 of 2.5. This increase in $\Delta P/q_{ref}$ with liner length is considered to be negligible for the range of variables investigated.

Effect of number of hole rows. - The preceding results were all obtained for 19 air-entry locations evenly distributed along the length of the combustor. The variation of $\Delta P/q_{ref}$ with the number of hole rows for values of exit to inlet total temperature ratio T_4/T_3 of 1.0 and 2.5 is shown in figure 12. The effect on $\Delta P/q_{ref}$ is negligible for about eight or more hole rows. For a lesser number of hole rows, $\Delta P/q_{ref}$ increases as the number of hole rows is decreased, because for a fewer number of hole rows the expansion loss in the annuli is greater. However, the effect is relatively small.

Effect of axial hole distribution. - The preceding results were obtained for an even distribution of liner hole area along the length of the combustor. The effect of changing the axial hole distribution from an even distribution to a distribution in which the accumulated open area increased parabolically with the square of the fractional length x/L was investigated for values of A_L/A_{ref} of 0.6, $A_{H,liner}/A_{ref}$ of 0.8, $A_{H,dome}/A_{H,liner}$ of 0.1, M_{ref} of 0.094, and T_4/T_3 of 1.0 and 2.5. The calculated values for $\Delta P/q_{ref}$ are slightly higher for the parabolic hole distribution. For a value of T_4/T_3 of 1.0, the values of $\Delta P/q_{ref}$ are 6.90 for the even hole distribution and 7.19 for the parabolic hole distribution. For a value of T_4/T_3 of 2.5, the values of $\Delta P/q_{ref}$ are 10.42 for the even hole distribution and 10.59 for the parabolic hole distribution. This variation in $\Delta P/q_{ref}$ is attributed to (1) an increase in expansion loss in the annuli and (2) an increase in the annulus wall friction due to higher velocities in the annulus for the parabolic hole distribution. In any event, the variation in $\Delta P/q_{ref}$ with axial hole distribution is relatively small.

Effect of proportionment of open hole area on inner and outer liner wall. - In the previous results, the open hole areas on the inner and outer liner wall were equal and the cross-sectional areas of the inner and outer annuli were equal. Figure 13 shows the variation of $\Delta P/q_{ref}$ with the ratio of the open hole area on the outer liner wall to the liner open hole area of both walls, $A_{H,liner,outer}/A_{H,liner}$ for values of T_4/T_3 of 1.0 and 2.5. The calculations were made for equal inner and outer annuli cross-sectional areas. Increasing the value of $A_{H,liner,outer}/A_{H,liner}$ above about 0.5 causes an increase in $\Delta P/q_{ref}$. The effect of shifting the proportion of airflow to the outer annulus without adjusting the cross-sectional area of the outer annulus is similar to the effect of increasing A_L/A_{ref}. The computation was then repeated by making the ratios of the cross-sectional areas of the outer and inner annuli equal to the ratios of the open hole areas. For this case, $\Delta P/q_{ref}$ was constant for all values of $A_{H,liner,outer}/A_{H,liner}$ and equal to the minimum value at $A_{H,liner,outer}/A_{H,liner}$ of 0.5.

Effect of varying liner cross-sectional area along length of combustor. - The results discussed thus far in this report have been for combustors with constant liner cross-sectional area along the length of the combustor. The effect of varying the ratio of liner cross-sectional area to combustor reference area, A_L/A_{ref}, along the length of the combustor on the total pressure loss coefficient is shown in figure 14. The value for A_L/A_{ref} was varied stepwise in three axial sections of equal length. Each of the three sections was

assigned a value of A_L/A_{ref} of 0.5, 0.6, or 0.7, while holding the average value of A_L/A_{ref} for the overall length at 0.6. The cross-sectional areas of the inner and outer annuli are equal at any given axial location. These data are compared with the previous data presented for the combustor with constant liner cross-sectional area. For the combinations of A_L/A_{ref} investigated, the total pressure loss coefficient is minimized by assigning the lowest values of A_L/A_{ref} at the front end of the combustor ($A_{L,1}/A_{ref}$ = 0.5, $A_{L,2}/A_{ref}$ = 0.6, $A_{L,3}/A_{ref}$ = 0.7), while the maximum value of $\Delta P/q_{ref}$ was obtained by assigning the highest values of A_L/A_{ref} at the front end of the combustor ($A_{L,1}/A_{ref}$ = 0.7, $A_{L,2}/A_{ref}$ = 0.6, $A_{L,3}/A_{ref}$ = 0.5). This trend is apparent for all of the cases shown even though the average value of A_L/A_{ref} for the overall length of the combustor was held at a constant value of A_L/A_{ref} = 0.6. It is interesting to note that the total pressure loss coefficient is lower for the case with ($A_{L,1}/A_{ref}$ = 0.5, $A_{L,2}/A_{ref}$ = 0.6, $A_{L,3}/A_{ref}$ = 0.7) than that for the constant values of A_L/A_{ref} = 0.5 or 0.6 and that the total pressure loss is higher for the case with ($A_{L,1}/A_{ref}$ = 0.7, $A_{L,2}/A_{ref}$ = 0.6, $A_{L,3}/A_{ref}$ = 0.5) than that for the constant value of A_L/A_{ref} = 0.7. These effects are attributed to the increase in the effective area of the air entry holes in the front portion of the liner as a result of an increase in the correlating flow parameter (fig. 8) as $A_{L,1}/A_{ref}$ is reduced. This is a direct result of the lowering of the velocities in the front portion of the annulus.

An extension of the results shown in the previous section was obtained for an annular combustor with conical inner and outer liner walls as shown in the schematic drawing in figure 15. The cross-sectional areas of the inner and outer annuli are equal at any given axial location. The cross-sectional area of the liner at the leading edge of the first hole row is designated as $A_{L,1}$. The air entry area is evenly spaced along the axis of the liner with the last hole row positioned at x/L = 0.95. The variation of $\Delta P/q_{ref}$ with $A_{L,1}/A_{ref}$ for various values of T_4/T_3 is shown in figure 15 for conical liner walls compared with cylindrical liner walls. For the cylindrical case, the value of A_L/A_{ref} is constant along the length of the combustor and equal to $A_{L,1}/A_{ref}$ however, for the conical case, the value of A_L/A_{ref} increases along the length of the combustor from a minimum value of $A_{L,1}/A_{ref}$ at the first hole row to a maximum value of about 0.95 at the last hole row where x/L = 0.95. The effect of wall inclination of the discharge coefficient of liner air-entry holes was ignored; however, this effect was shown to be small in reference 6. For conical liner walls, the value of $\Delta P/q_{ref}$ approaches a minimum as the value of $A_{L,1}/A_{ref}$ approaches zero for T_4/T_3 of 1.0 and the value of $\Delta P/q_{ref}$ is a minimum at a value of $A_{L,1}/A_{ref}$ of about 0.3 for T_4/T_3 of 3.0. The value of $\Delta P/q_{ref}$ for the conical geometry is lower than that for the cylindrical geometry when $A_{L,1}/A_{ref}$ is below a value of about 0.5 for T_4/T_3 of 1.0. Similar trends were shown previously in reference 7 for a tubular combustor with a conical liner. Practical considerations in the designs of the primary zone, and secondary mixing zone usually preclude the use of conical liner walls despite the apparently lower value of $\Delta P/q_{ref}$.

Effect of combustor outer diameter. - In the preceding results, the combustor outer diameter was assumed to be 40 inches (1.016 m) and the inner diameter was assumed to be 20 inches (0.508 m). Limited calculations were performed for outer diameters of 30 inches (0.762 m) and 60 inches (1.524 m) with the inner diameter held at 20 inches (0.508 m) and combustor length held at 20 inches (0.508 m) for values of A_L/A_{ref} of 0.6, $A_{H,liner}/A_{ref}$ of 0.8, $A_{H,dome}/A_{H,liner}$ of 0.1, M_{ref} of 0.904, and T_4/T_3 of 1.0 and 2.5. It is to be expected that the only significant effect of increasing the combustor outer diameter is to reduce the total pressure loss from wall friction in the annulus due to the increased values for the hydraulic radius of the inner and outer annuli. The calculated values of $\Delta P/q_{ref}$ for outer diameters of 30, 40, and 60 inches (0.762, 1.016, and 1.524 m) were 6.98, 6.90, and 6.86, respectively, for T_4/T_3 of 1.0, and 10.49, 10.40, and 10.40, respectively, for T_4/T_3 of 2.5. The expected trend is apparent from the results but the change is small.

Combustor Airflow Distribution

Effect of liner open hole area. - In figure 16 the combustor airflow distribution is shown as the variation of the fraction of the total airflow passing through the liner at any given axial location, W_L/W_T with the fraction of liner open hole area up to that location, $A_H/A_{H,liner}$ for various values of $A_{H,liner}/A_{ref}$ at a value of $A_{H,dome}/A_{H,liner} = 0$. At a value of $A_{H,liner}/A_{ref}$ of 0.4, W_L/W_T is approximately linear with $A_H/A_{H,liner}$ at all positions along the length of the combustor; however, as $A_{H,liner}/A_{ref}$ increases the fraction of air entering the upstream air entry holes in the liner decreases. The decrease in W_L/W_T for air entry holes in the upstream portion of the liner is a result of a proportionately larger reduction in pressure drop and discharge coefficients for these holes. These trends are similar to those shown previously for the tubular combustor in reference 3.

In figure 17, airflow distribution curves are presented for a value of $A_{H,dome}/A_{H,liner}$ of 0.1. The combustor dome is located at a value of $A_H/A_{H,liner} = 0$. The fraction of airflow through the combustor dome increases as the value for $A_{H,liner}/A_{ref}$ increases; the increase in flow through the dome is relatively small for values of A_L/A_{ref} of 0.5 and 0.6, but becomes greater at values of A_L/A_{ref} of 0.7 and 0.85.

Effect of combustor reference Mach number. - The effect of reference Mach number on airflow distribution is shown in figure 18. Increasing the reference Mach number decreases the proportion of flow through the front end of the combustor; however, for the range of M_{ref} studied the effect is shown to be small for a T_4/T_3 of 3.0 and is shown to be negligible for a T_4/T_3 of 1.0.

Effect of heat release. - The effect of exit to inlet total temperature ratio T_4/T_3 on combustor airflow distribution is shown in figure 19 for values of $A_{H,liner}/A_{ref}$ of 0.4

and 1.0. The decrease in the fraction of airflow entering the liner through upstream holes with increasing values of T_4/T_3 is more pronounced for the larger value of $A_{H,liner}/A_{ref}$. The reduction in upstream liner airflow is substantial for increases in T_4/T_3 up to about 3.0 but further increases in T_4/T_3 from 3.0 to 4.0 result in only small reductions in upstream liner airflow. The effect of T_4/T_3 on the airflow distribution decreases as A_L/A_{ref} increases from 0.5 to 0.85.

Effect of liner cross-sectional area. - The effect of A_L/A_{ref} on combustor airflow distribution is shown in figure 20 for values of $A_{H,liner}/A_{ref}$ of 0.4 and 1.0. At a value of T_4/T_3 of 1.0 increasing A_L/A_{ref} from 0.5 to 0.7 results in a small reduction in airflow through the upstream liner holes and a small increase in airflow through the combustor dome; further increases in A_L/A_{ref} from 0.7 to 0.85 results in a more substantial reduction in airflow through the upstream liner holes and a larger increase in airflow through the combustor dome. These effects are more pronounced at the larger value of $A_{H,liner}/A_{ref}$. At a value of T_4/T_3 of 3.0, the effect of A_L/A_{ref} on airflow distribution is similar to that shown for a T_4/T_3 of 1.0. The effects are more pronounced however, at a $T_4/T_3 = 3.0$.

Effect of open area in the combustor dome. - The effect of $A_{H,dome}/A_{H,liner}$ on the combustor airflow distribution is shown in figure 21. The values presented for $A_{H,dome}/A_{H,liner}$ of 0, 0.1, 0.2, and 0.4 correspond to values of $A_{H,dome}/A_{H,total}$ (ratio of open area in dome to total open area in dome and liner) of 0, 0.091, 0.167, and 0.286, respectively. Increasing $A_{H,dome}/A_{H,liner}$ results in a proportionately larger increase in airflow through the combustor dome and decrease in airflow through the upstream holes. This occurs because as $A_{H,dome}/A_{H,liner}$ increases, the discharge coefficients become relatively lower for the air entry holes in the upstream portion of the liner.

Effect of liner air entry geometry. - The effect of liner hole geometry on combustor airflow distribution is shown in figure 22 in which data for a 3/4-inch (0.019-m) diameter flush hole are compared with data for a scoop over a flush hole with a value of face area to flush hole area of 1.378. As expected from the higher discharge coefficient for the scoop, the fractional airflow through the upstream holes in the liner increases with the use of the scoop; however, this effect is accompanied by a proportional decrease in flow through the dome.

Effect of a varying liner cross-sectional area along length of combustor. - The effect of varying the ratio of liner cross-sectional area to combustor reference area, A_L/A_{ref}, along the length of the combustor on the liner airflow distribution is shown in figure 23. The value for A_L/A_{ref} was varied stepwise in three axial sections of equal length. Each of the three sections had a value of A_L/A_{ref} of 0.5, 0.6, or 0.7 while holding the average value of A_L/A_{ref} for the overall length at 0.6. Liner airflow distribution curves are presented for the varying liner cross-sectional areas that had the highest and lowest total pressure loss coefficients in figure 8 and are compared with the liner airflow distri-

bution of the combustor with a constant liner cross-sectional area ratio of 0.6. The liner that had the lowest total pressure loss coefficient ($A_{L,1}/A_{ref} = 0.5$, $A_{L,2}/A_{ref} = 0.6$, and $A_{L,3}/A_{ref} = 0.7$) also had the most nearly linear airflow distribution. And the liner with the highest total pressure loss coefficient ($A_{L,1}/A_{ref} = 0.7$, $A_{L,2}/A_{ref} = 0.6$, and $A_{L,3}/A_{ref} = 0.5$) had a liner airflow distribution deviating most from linearity. The sudden change in slopes in the curves correspond to where the liner cross-sectional area changes.

The effect of conical inner and outer walls on liner airflow distribution is shown in figure 24 in which conical liner walls with values of $A_{L,1}/A_{ref}$ of 0.1, 0.4, and 0.5 are compared with cylindrical liner walls with an A_L/A_{ref} of 0.6. The airflow through the upstream portion of the liner is higher for the conical liner than the cylindrical liner and increases slightly with increases in $A_{L,1}/A_{ref}$. Similar results were reported for tubular combustors with conical liners in reference 7.

Effect of other variables. - The effect of other variables including liner length, number of hole rows, axial hole distribution, proportionment of hole area on inner and outer liner wall, combustor diameter, and film cooling slots on combustor airflow distribution were analyzed for values of A_L/A_{ref} of 0.6, $A_{H,liner}/A_{ref}$ of 0.8, $A_{H,dome}/A_{H,liner}$ of 0.1, M_{ref} of 0.094 and T_4/T_3 of 1.0 and 2.5. None of these variables significantly effect airflow distribution.

COMPARISON OF CALCULATED RESULTS FOR ANNULAR COMBUSTOR WITH TUBULAR COMBUSTOR

The analytical results obtained for the tubular combustor in reference 3 should be applicable to the annular combustor with parallel walls and flush liner hole openings if the velocities in the inner and outer annuli are equal at any axial location along the length of the combustor. Slight differences arise from the differences in hydraulic radius and the calculation of expansion losses in the annulus. Selected results from this report are compared in this section with the results of reference 3. The variation of the total pressure loss coefficient with $A_{H,liner}/A_{ref}$ obtained from analytical data for the annular combustor and tabular combustor (ref. 3) is compared in figure 25. These data are compared for values of A_L/A_{ref} of 0.6, no dome flow and isothermal conditions. The calculated annular combustor data were obtained for a value of M_{ref} of 0.031 while the calculated tabular combustor data were obtained for incompressible flow; however, the effect of Mach number at this level is negligible. The data in figure 25 agree quite well.

In figure 26 a comparison is made of the variation of $\Delta P/q_{ref}$ with reference Mach number for the two sets of data. The data are compared for an $A_{H,liner}/A_{ref} = 0.8$, no dome flow and isothermal conditions and A_L/A_{ref} of 0.5, 0.6, and 0.7. Figure 26

shows that M_{ref} has a greater influence on $\Delta P/q_{ref}$ for the tubular data than for the annular data; however, the agreement between the two sets of data is satisfactory.

In figure 27 a comparison is made of the variation of $\Delta P/q_{ref}$ with T_4/T_3. The data are compared for an A_L/A_{ref} of 0.6, $A_{H,liner}/A_{ref}$ of 0.8, $A_{H,dome}/A_{H,liner}$ of 0, and for M_{ref} of 0.031 and 0.094 in the annular data and for $M_{ref} = 0$ (incompressible flow) in the tubular data. Figure 27 shows that the agreement between the two sets of data is satisfactory if the effects of M_{ref} is accounted for.

In figure 28, the airflow distributions are compared for the two sets of data for A_L/A_{ref} of 0.6, no dome flow and isothermal conditions with a value of M_{ref} of 0.063 for the annular data and with a value of M_{ref} of 0.05 for the tubular data. Figure 28 shows satisfactory agreement between the airflow distribution curves for the two sets of data.

APPLICATION TO COMBUSTOR DESIGN

The combustor total pressure loss coefficient and airflow distribution for a given annular combustor design may be estimated from the curves provided in the report by determining the dimensionless parameters $A_{H,liner}/A_{ref}$, A_L/A_{ref}, $A_{H,dome}/A_{H,liner}$, M_{ref}, and T_4/T_3. In general, the effects of other variables such as combustor length, number of hole rows, axial hole distribution, and combustor outer diameter, may be ignored without introducing any significant errors in these estimates. Most of the curves presented pertain to flush air entry ports in the liner. A rough estimate of the total pressure loss coefficient for liners with scoops may be obtained from figure 10. The actual total pressure for a liner with a given scoop geometry may be obtained by multiplying the ratio of $\Delta P/q_{ref}$ for the scoop to $\Delta P/q_{ref}$ for the flush hole obtained from figure 10 for given values of $A_{H,liner}/A_{ref}$ and T_4/T_3 by the $\Delta P/q_{ref}$ data for flush air entry holes. The influence of film cooling slots on $\Delta P/q_{ref}$ may be estimated from figure 11.

The results associated with figure 13 would indicate that the data presented with equal cross-sectional areas for inner and outer annuli should be representative for combustors with unequal cross-sectional areas for inner and outer annuli as long as the hole area in the inner and outer liner wall is proportional to the respective cross-sectional areas of the annuli. For combustors in which liner cross-sectional area varies along the combustor length the results from figures 14 or 15 may be used to estimate the total pressure loss. For annular combustors with greatly varying values of A_L/A_{ref} along the length of the combustor, specific computations using the program of reference 1 may be necessary to obtain satisfactory estimates.

CONCLUDING REMARKS

The calculated total pressure loss and airflow distribution data presented in this report for the annular combustor agreed quite well with comparable calculated data from a previous report on the tubular combustor. Some significant extensions to the previously available data are as follows: an increased range of open hole area in the dome, the combined effect of combustor reference Mach number and heat release, the use of a liner hole with a scoop, and the use of a liner in which the cross-sectional area varies with combustor length. The curves presented in this report may be used to make preliminary combustor design estimates. The report has shown that the computer program is a useful tool for making preliminary combustor design estimates, and may be used to obtain more detailed data for specific combustor designs that are not covered by the generalized curves of this report.

Lewis Research Center,
National Aeronautics and Space Administration,
Cleveland, Ohio, June 2, 1969,
120-03-00-89-22.

APPENDIX A

SYMBOLS

A	area
A_{an}	cross-sectional area of annulus
A_c	total face area of cooling slots
A_f	face area of scoops
A_H	liner open hole area from dome to x
$A_{H,dome}$	open area in liner dome including openings in liner dome and swirler
$A_{H,liner}$	open hole area in liner walls (excluding liner dome openings)
$A_{H,liner,outer}$	open hole area in outer liner wall
$A_{H,total}$	total open hole area in both dome and liner wall
A_h	flush area of hole
A_L	cross-sectional area of liner
$A_{L,1}$	cross-sectional area of liner at first hole row
A_{ref}	reference area; total combustor cross-sectional area between combustor inner and outer diameter
A_w	wetted wall area per unit length
C_d	orifice discharge coefficient, ratio of measured to theoretical flow through hole
C_p	orifice discharge coefficient, corrected for pressure ratio effect
c_p	specific heat at constant pressure
F	Fanning friction factor
g_o	gravitational constant, 32.2 ft/sec^2
h	enthalpy
K_{sw}	constant, swirler equation
L	length of combustor
M	Mach number
$\dot{m}_{fb}$	mass flow rate of fuel burned
P	total pressure
p	static pressure
ΔP	total pressure loss across combustor, $P_4 - P_3$
ΔP_{1-2}	change in total pressure due to heat addition in primary zone

$\Delta P/q_{ref}$	combustor total pressure loss coefficient
$\dot{q}$	heat transfer rate
q_{ref}	reference dynamic pressure; $\frac{W_T^2}{2g\rho_{st,3}} A_{ref}^2$; $\frac{\gamma_a}{2} p_3 M_{ref}^2$
Re	Reynolds number
T	total temperature
u	velocity
W	mass flow rate passing through any given passage
W_h	mass flow rate passing through liner holes
W_L	mass flow rate passing through combustor liner
W_T	total mass flow rate passing through combustor
x	distance along combustor axis measured from dome
β_{sw}	angle of swirler blades
γ_a	specific heat ratio of air
ρ	density
$\rho_{st,3}$	density at station 3 based on static pressure and static temperature
φ	jet angle

Subscripts:

an	annulus
dome	liner dome
h	liner hole
j	air jet from liner hole
L	liner
sw	swirler
ref	reference
1	conditions at current axial station just before liner wall hole
1'	conditions at current axial station just after liner wall hole
2	conditions at axial location downstream of liner wall hole
3	combustor inlet
4	combustor exit

APPENDIX B

CALCULATION PROCEDURES

The combustor total pressure loss coefficient and liner airflow distribution are obtained from assigned values of combustor geometry and operating conditions. The static pressure, total pressure, total temperature, and velocity along the inner and outer annuli and along the liner are also obtained from the calculations. The required input information on combustor geometry includes the coordinates of the inner and outer annuli and the liner along the combustor length and the size, shape, and location of all air entry ports. The required operating data includes the combustor inlet airflow, inlet total pressure, inlet total temperature, and the fuel-air ratio.

The computation begins with an initial estimate of the fraction of the inlet airflow that passes through the inner and outer annuli and the combustor dome. The static pressure in the primary zone of the liner is then calculated from the inlet total pressure and the estimated flow through the combustor dome from the relation

$$W_h = C_d A_h \left[2 g_o \rho_{an} (P_{an} - p_L)\right]^{1/2} \tag{1}$$

where P_{an} and ρ_{an} are at the combustor inlet conditions since the diffuser and snout have not been included in these calculations. The discharge coefficient, C_d, for all openings in the combustor dome was assumed to be 0.6. A comparison calculation was made for one case using the following relation for flow through a swirler from reference 8:

$$\frac{P_{an} - p_L}{q_{ref}} = K_{sw} \left(\frac{A_{ref}^2}{A_{sw}^2} \sec^2 \beta_{sw} - \frac{A_{ref}^2}{A_L^2} \right) \frac{W_{sw}^2}{W_{total}^2} \tag{2}$$

The constants K_{sw} and β_{sw} were assumed to be 1.3 and 50 degrees, respectively. Equations (1) and (2) were in reasonable agreement on the calculated value for static pressure in the primary zone. In the absence of more precise experimental data for discharge coefficients of combustor dome air entry ports such as swirlers, the use of equation (1) with a C_d value of 0.6 was considered to be a reasonable assumption.

The air entry ports in the inner and outer annuli are assigned axial station numbers as shown in figure 29. The airflow, static and total pressures, total temperature, and velocity are obtained at each station from a solution of the equations of momentum, energy, continuity, and state for the inner and outer annuli and the liner using as the input, conditions from the previous station. Experimental values of discharge coefficients

are used from references 5 and 6.

The computation of airflow through each air entry port station in the liner is repeated stepwise from the front to the rear of the combustor. If the accumulated airflow through the liner differs from the combustor inlet airflow rate, the entire computation is repeated until convergence is obtained using reassigned values for the fraction of inlet airflow that passes through the inner and outer annuli and the combustor dome.

Primary Zone Calculations

The primary zone is assumed to be a stirred reactor with a uniform pressure, temperature, and fuel-air ratio, where mixing and burning occur instantaneously. For the data presented in RESULTS AND DISCUSSION, the primary zone was arbitrarily defined as ending at the first hole row in the liner wall. The effect of altering the position of the end of the primary zone was investigated for a representative geometry with fixed operating conditions and hole pattern. These results are presented in figure 30 which shows the variation of the combustor total pressure loss coefficient with fractional length of primary zone. The total pressure loss is fairly insensitive for primary zone lengths up to one-half the combustor length beyond which the total pressure loss is greatly reduced. From a consideration of $\Delta P/q_{ref}$ only, the choice of primary zone length used for the calculations herein appears to be satisfactory.

Part of the airflow entering the first hole row in the liner is assumed to recirculate into the primary zone. The amount of air that recirculates was calculated from the following empirical expression based on experimental data for a tubular combustor from reference 9.

$$\text{Fraction of air that recirculates} = 0.5 \sin \varphi \left(\frac{T_{an}}{T_L}\right)^{1/2} \tag{3}$$

φ is the jet angle which is calculated from data correlations and local conditions in the annulus and liner. Recirculation of airflow into the primary zone from other liner air entry stations is assumed to be zero. A limited number of calculations were made in which the fraction of air from the first hole row that recirculates into the primary zone was arbitrarily chosen instead of using equation (3). Fractions from 0 to 1.0 resulted in a negligible change in the total pressure loss coefficient.

The energy equation for combustion in the primary zone has the following form:

$$W_{air,1} h_{air,T_1} + \dot{q} = (W_{air,1} + \dot{m}_{fb}) h_{prod,T_2} \tag{4}$$

The subscripts 1 and 2 used here refer to conditions before and after combustion. Velocity terms were neglected because the velocity in the primary zone is assumed to be low. The enthalpies of air and combustion products were calculated from the expression:

$$h = \int c_p \, dT \tag{5}$$

The specific heat of combustion products were corrected for dissociation effects. A fuel lower heating value of 18 540 Btu per pound (4.311×10^7 J/kg) and a fuel hydrogen-carbon ratio of 0.17 were used.

The total pressure loss due to heat addition in the primary zone is obtained from

$$\Delta P_{1-2} = \frac{\rho_2 u_2^2}{2g_o} \left(1 - \frac{\rho_2}{\rho_1}\right) \tag{6}$$

Annulus Calculations

The equations of momentum, energy, continuity, and state are solved for stepwise increments along the length of both the inner and outer annuli. The calculated total pressure loss in each annulus includes the effects of the following:

(1) Sudden expansion losses in the annulus occurring downstream of each air entry port in the liner

(2) Annulus wall friction

The total pressure loss due to sudden expansion is obtained from the following empirical expression:

$$P_{an,1} - P_{an,1'} = 1.85 \frac{\rho_{an,1} u_{an,1}^2}{2g_o} \left(\frac{W_h}{1.36 \, W_{an,1}}\right)^{1/\left(0.5+0.242 \, M_{an,1}^{2.21}\right)} \tag{7}$$

This expression was obtained from references 1 and 2 by fitting the curves from reference 11. The total pressure loss due to wall friction is obtained from the momentum equation for the annulus using the following:

$$p_{an,1}A_{an,1} + \frac{W_{an,2}u_{an,1'}}{g_o} + \int_{x_1}^{x_2} p_{an}\frac{dA_{an}}{dx}\,dx - \int_{x_1}^{x_2} \frac{FA_w u_{an}^2}{2g_o}\,dx$$

$$= p_{an,2}A_{an,2} + \frac{W_{an,2}u_{an,2}}{g_o} \qquad (8)$$

where $F = 0.0035 + 0.264\,Re_{an,1}^{-0.42}$ (ref. 11).

Liner Calculations

The momentum equation for the liner can be written as follows:

$$p_{L,1}A_{L,1} + \frac{W_{L,1}u_{L,1}}{g_o} + \frac{(A_{L,2} - A_{L,1})(p_{L,1} + p_{L,2})}{2} + \sum_{\text{Entering jets}} W_{j,o}u_{j,o}\cos\varphi_{j,o}$$

$$+ \sum_{\text{Residual jets}} W_{j,1}u_{j,1}\cos\varphi_{j,1} = p_{L,2}A_{L,2} + \frac{W_{L,2}u_{L,2}}{g_o}$$

$$+ \sum_{\text{All jets}} W_{j,2}u_{j,2}\cos\varphi_{j,2} \qquad (9)$$

where φ_j equals local angle between jet axis and liner centerline and W_L equals mass flow of hot gases (excludes unmixed air in residual jets but includes mass of fuel burned between stations 1 and 2).

Jet Mixing

The computer program contains four different jet mixing models to predict the rate at which the penetration or wall jets mix into the liner gas stream. They are referred to as the mass loss, the equivalent entrainment, the profile substitution, and the instantaneous mixing models. Each of the mixing models is briefly described below; however, a more detailed discussion is contained in references 1 and 2.

In the mass loss model a specified fraction of the initial mass flow in the jet is assumed to mix with the main gas stream for each unit of distance along the jet. The equivalent entrainment model starts with the actual mass flow across the jet at a location downstream of the jet hole. This mass flow minus the initial mass flow through the hole is the mass flow of gases that have been entrained into the jet from the main stream. A fraction of this entrained gas is then assumed to mix with the main stream. The profile substitution model uses the transverse temperature profile of the jet to determine the jet boundary. The boundary is defined to be the points where the temperature of the gases in the jet stream is a specified fraction of the temperature at the jet inlet. Air outside the boundary is assumed to have mixed with the main stream. The instantaneous mixing model simply has the jets mix instantaneously with the main stream.

The use of each of the mixing models requires the use of an assumed constant. The rate of mixing increases as the value of the constant increases. In figure 31, the effect of the various mixing models and the constants on the total pressure loss coefficient is shown for a typical combustor. It is seen that except at the very low values of the constants the effect of the constant and the mixing method has little effect on $\Delta P/q_{ref}$. Instantaneous mixing was assumed to calculate the results presented in this report.

Static and Total Pressure Variation Along the Length of the Combustor

Figure 32 shows the calculated variation of the static and total pressures in the annulus and liner along the length of a typical annular combustor. The pressures are expressed as a fraction of the inlet total pressure. The value of the correlation flow parameter for liner air entry ports as a function of combustor length was calculated from the data of figure 32 and is shown in figure 33. The variation of the flow parameter results in lower discharge coefficients at the upstream end of the combustor liner. Similar trends were found for the tubular combustor in reference 3.

REFERENCES

1. Anon.: Computer Program for the Analysis of Annular Combustors. Vol. 1: Calculation Procedures. Rep. 1111-1, vol. 1, Northern Research and Engineering Corp. (NASA CR-72374), Jan. 29, 1968.

2. Anon.: Computer Program for the Analysis of Annular Combustors. Vol. 2: Operating Manual. Rep. 1111-2, vol. 2, Northern Research and Engineering Corp. (NASA CR-72375), Jan. 29, 1968.

3. Graves, Charles C.; and Grobman, Jack S.: Theoretical Analysis of Total-Pressure Loss and Airflow Distribution for Tubular Turbojet Combustors with Constant Annulus and Liner Cross-Sectional Areas. NACA Rep. 1373, 1958.

4. Sovran, Gino; and Klomp, Edward D.: Experimentally-Determined Optimum Geometries for Rectilinear Diffusers with Rectangular, Conical or Annular-Cross-Section. Fluid Mechanics of Internal Flow. Gino Sovran, ed., Elsevier Publ. Co., 1967, pp. 270-319.

5. Dittrich, Ralph T.; and Graves, Charles C.: Discharge Coefficients for Combustor-Liner Air-Entry Holes. I-Circular Holes with Parallel Flow. NACA TN 3663, 1956.

6. Dittrich, Ralph T.: Discharge Coefficients for Combustor-Liner Air-Entry Holes. II-Flush Rectangular Holes, Step Louvers, and Scoops. NACA TN 3924, 1958.

7. Grobman, Jack S.: Comparison of Calculated and Experimental Total-Pressure Loss and Airflow Distribution in Tubular Turbojet Combustors with Tapered Liners. NASA Memo 11-26-58E, 1959.

8. Knight, H. A.; and Walker, R. B.: The Component Pressure Losses in Combustion Chambers. ARC R&M 2987, 1957.

9. Rosenthal, J.: Exploratory Methods for the Determination of Gas Flow and Temperature Patterns in Gas Turbine Combustors. Mech. Eng. Note 235, Aeronautical Research Lab., Dept. of Supply, Australia, July 1959.

10. Anon.: Flow Through a Sudden Enlargement in a Pipe. Aerodynamics Data Sheet 00.03.29, Royal Aeronautical Soc., London, Jan. 1964.

11. Wilson, Robert E.; McAdams, W. H.; and Seltzer, M.: The Flow of Fluids through Commercial Pipe Lines. Ind. Eng. Chem., vol. 14, no. 2, Feb. 1922, pp. 105-119.

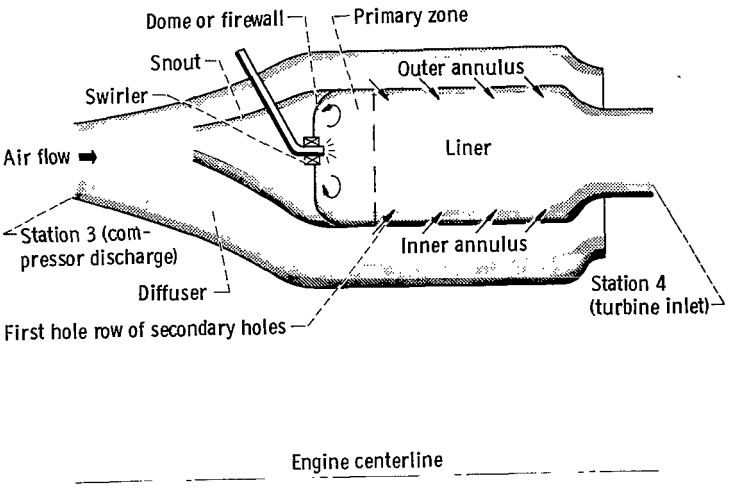

Figure 1. - Annular combustor cross-section.

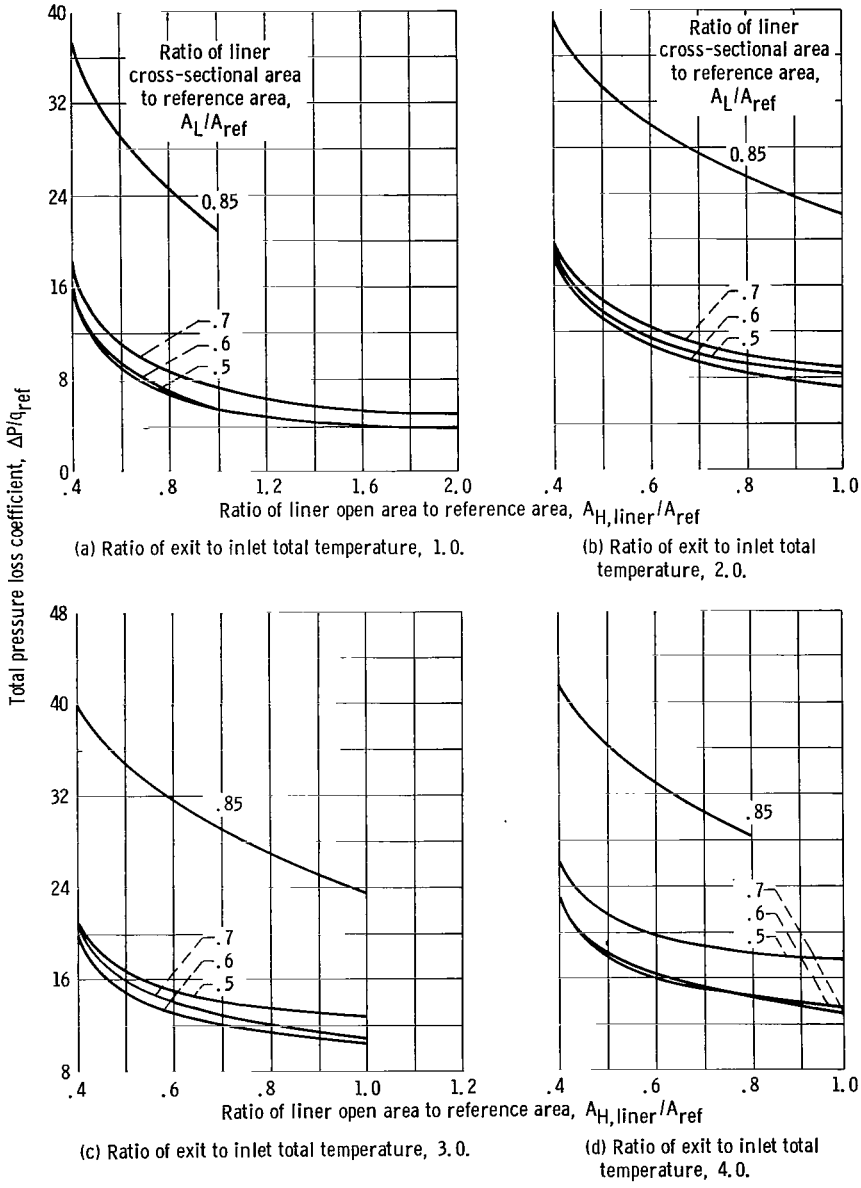

Figure 2. - Effect of liner open area on total pressure loss coefficient. Ratio of open area in dome to open area in liner, 0.1; reference Mach number, 0.063.

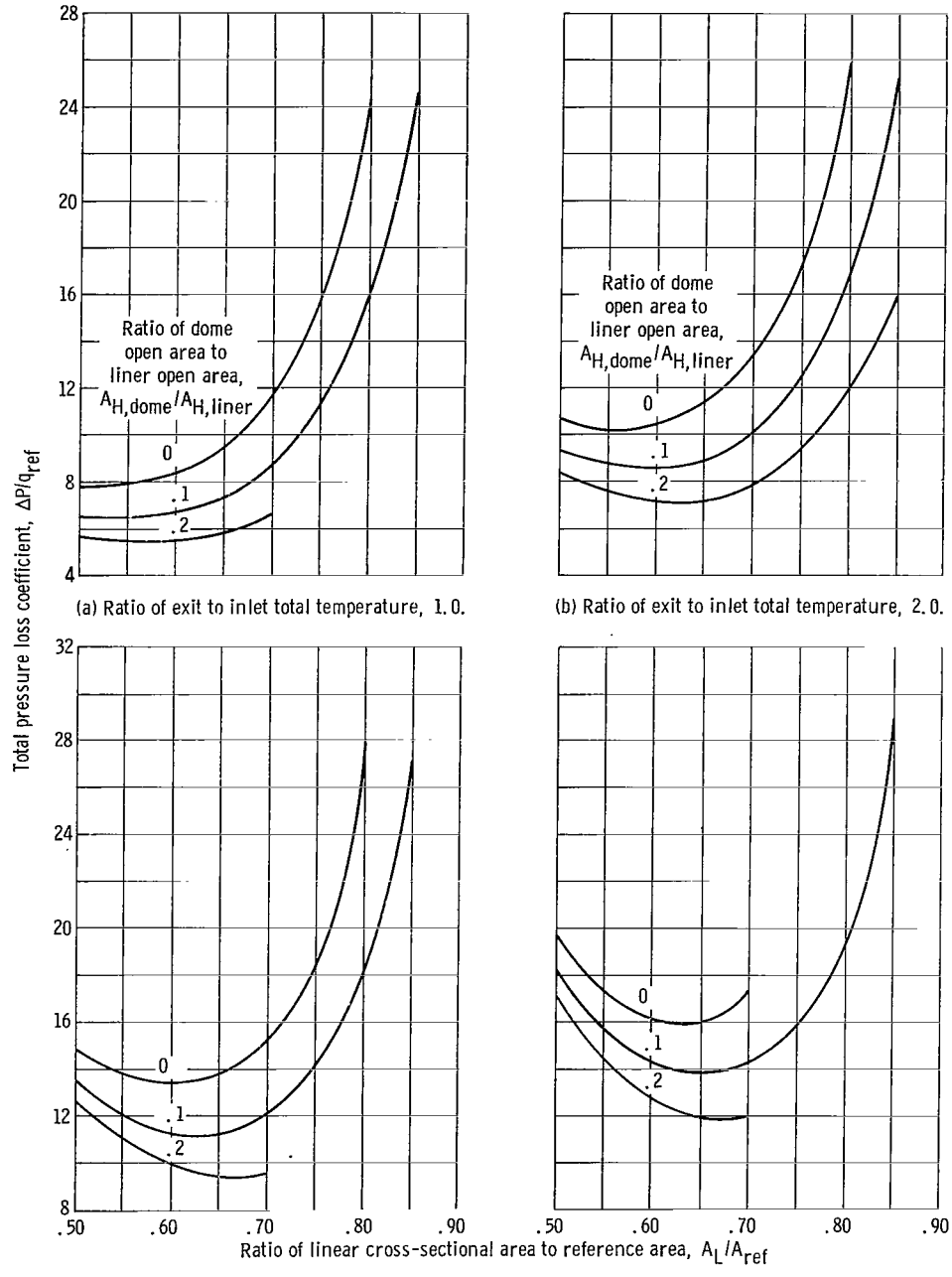

Figure 3. - Effect of liner cross-sectional area on total pressure loss coefficient. Ratio of liner open hole area to reference area, 0.8; reference Mach number, 0.063.

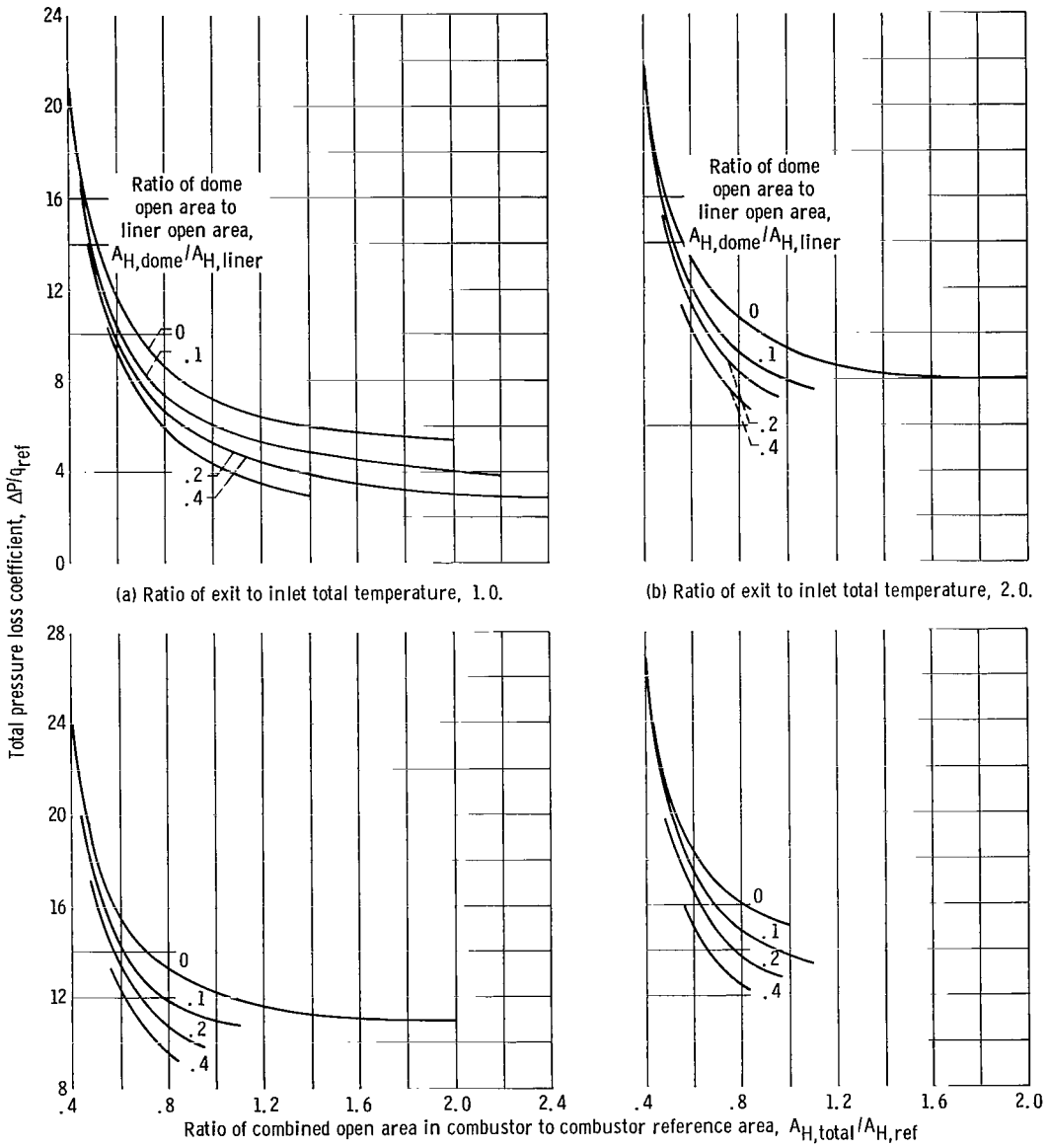

Figure 4. - Effect of total open hole area on total pressure loss coefficient. Ratio of liner cross-sectional area to reference area, 0.6; reference Mach number, 0.063.

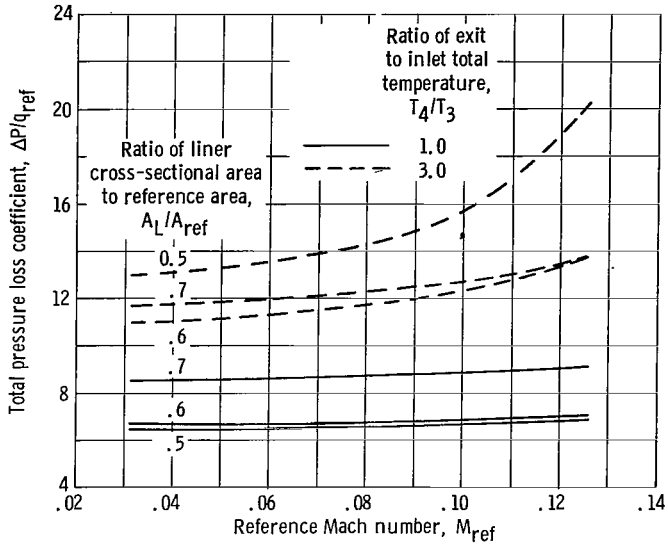

Figure 5. - Effect of reference Mach number on total pressure loss coefficient. Ratio of dome open area to liner open area, 0.1; ratio of liner open area to reference area, 0.8.

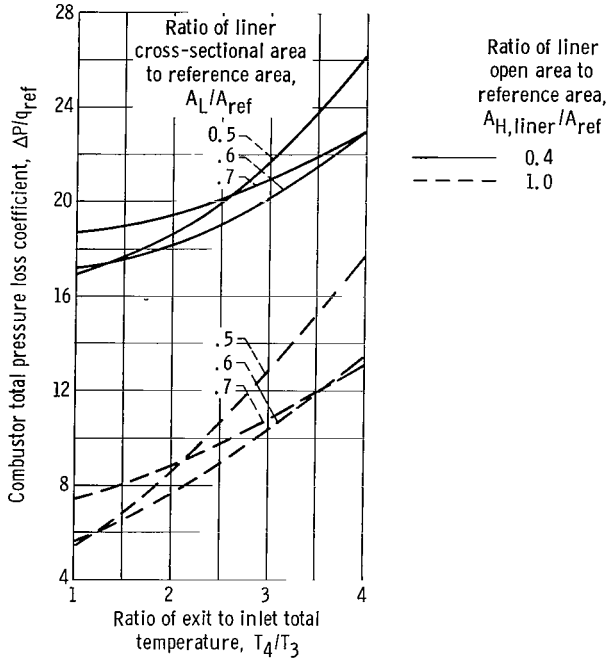

Figure 6. - Effect of heat release on total pressure loss coefficient. Ratio of dome open area to liner open area, 0.1; reference Mach number, 0.063.

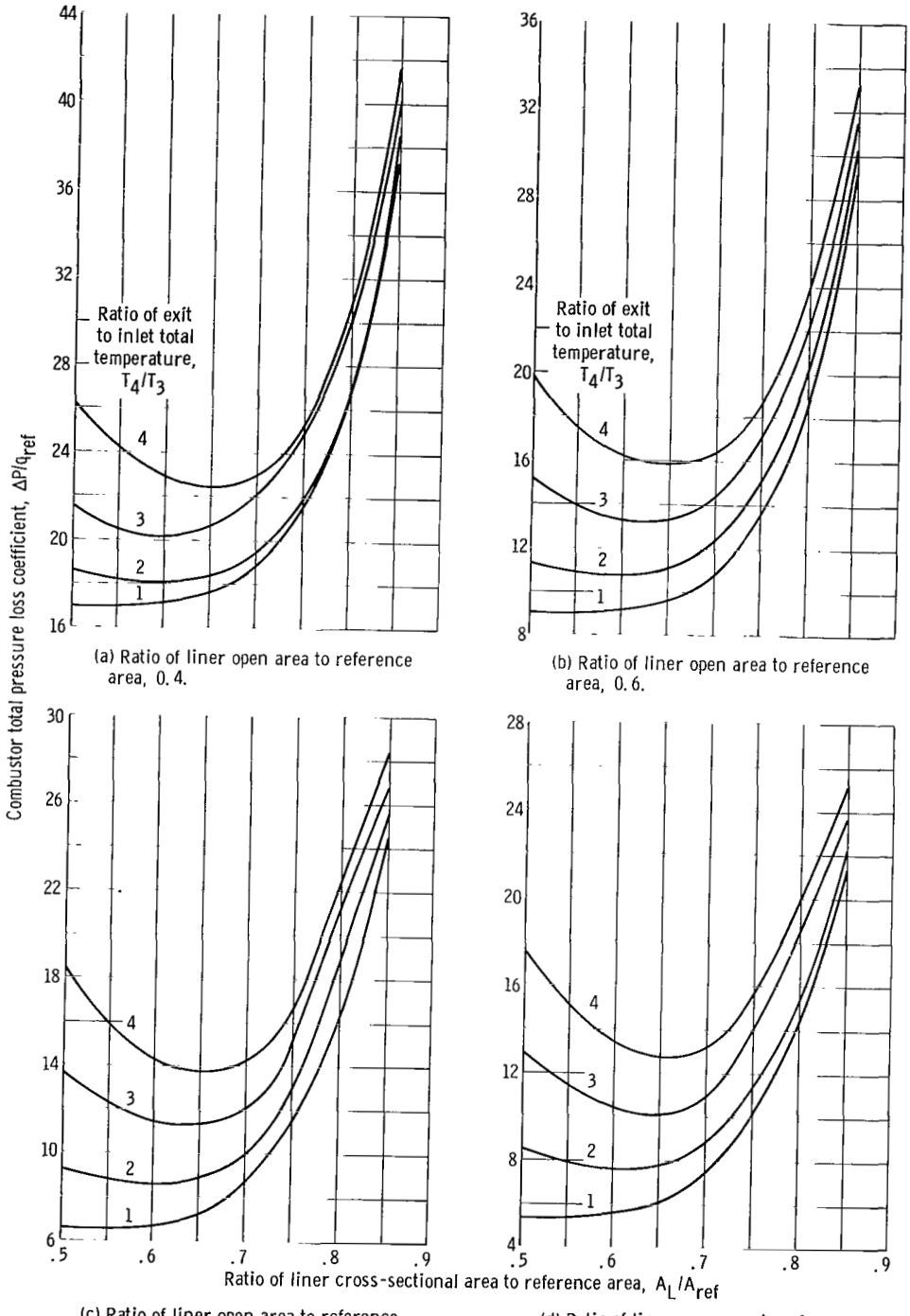

(a) Ratio of liner open area to reference area, 0.4.

(b) Ratio of liner open area to reference area, 0.6.

(c) Ratio of liner open area to reference area, 0.8.

(d) Ratio of liner open area to reference area, 1.0.

Figure 7. - Effect of heat release on variation of total pressure loss coefficient with ratio of liner cross-sectional area to reference area. Ratio of dome open area to liner open area, 0.1; reference Mach number, 0.063.

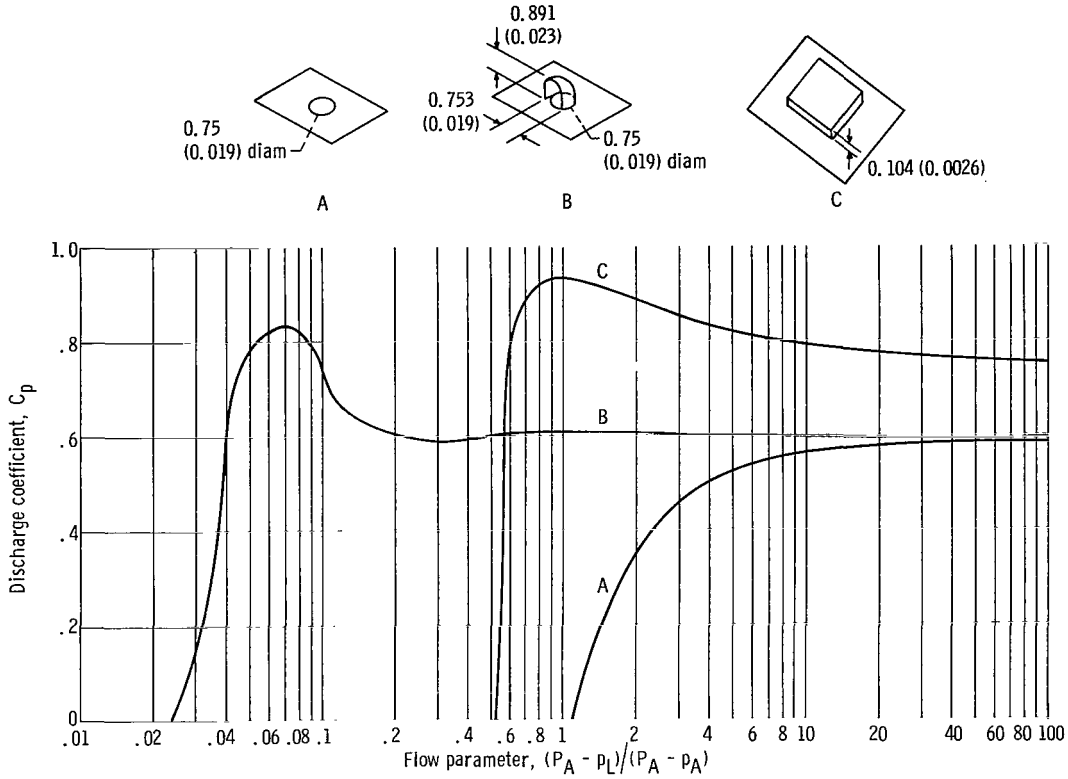

Figure 8. - Effect of flow parameter on discharge coefficient (corrected to a static pressure of unity) for various hole geometries (figs. from refs. 5 and 6). (Sketch dimensions are in inches (m).)

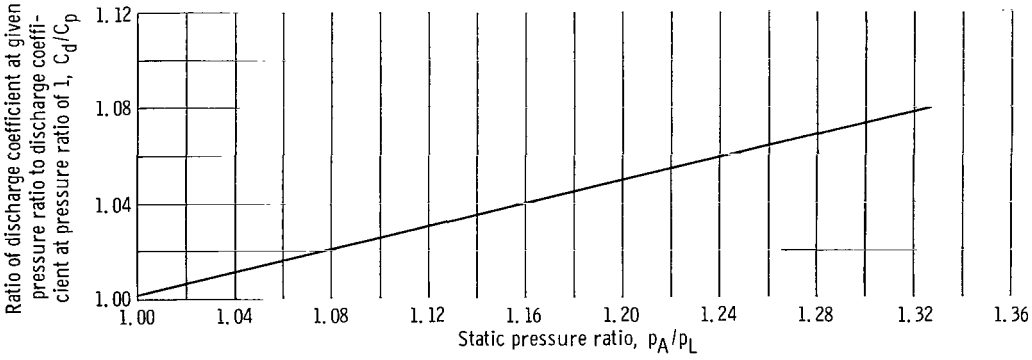

Figure 9. - Pressure-ratio correction factor for hole discharge coefficients (fig. from ref. 5).

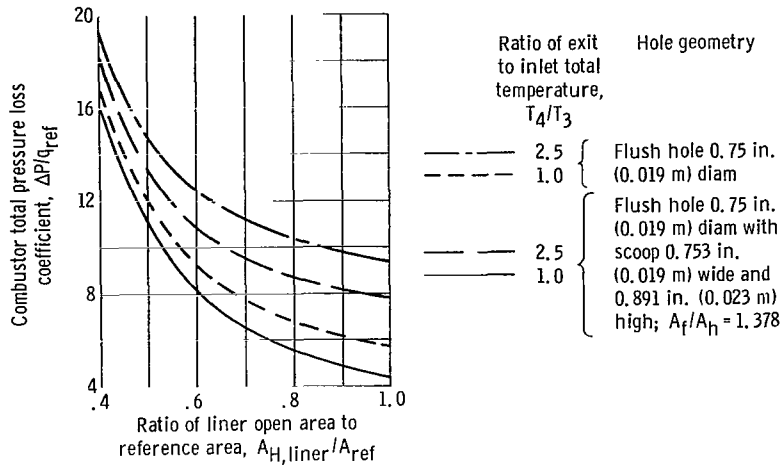

Figure 10. - Effect of liner hole geometry on total pressure loss coefficient. Liner cross-sectional area to reference area, 0.6; ratio of dome open area to liner open area, 0.1; reference Mach number, 0.094.

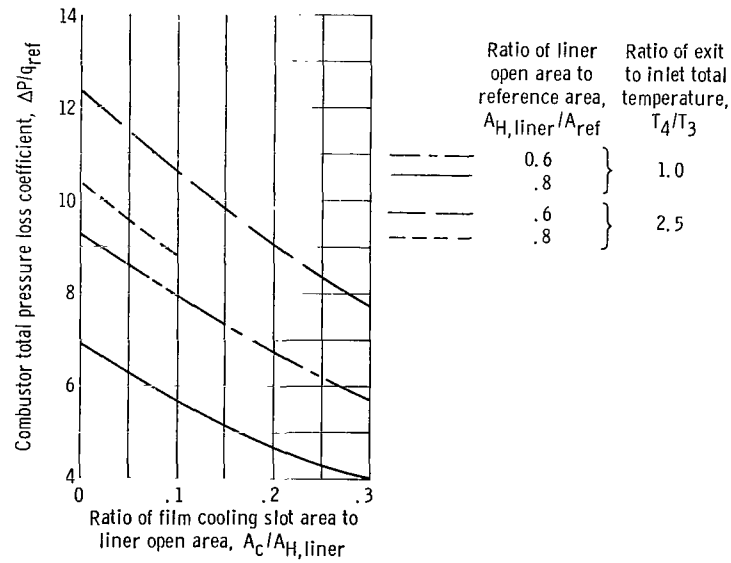

Figure 11. - Effect of film cooling slot area on total pressure loss coefficient. Ratio of liner cross-sectional area to reference area, 0.6; ratio of dome open area to liner open area, 0.1; reference Mach number, 0.063.

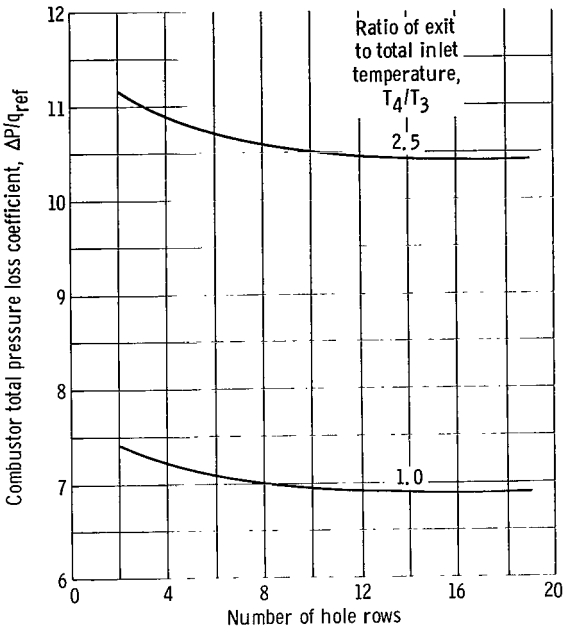

Figure 12. - Effect of number of hole rows on total pressure loss coefficient. Ratio of liner cross-sectional area to reference area, 0.6; ratio of liner open area to reference area, 0.8; ratio of dome open area to liner open area, 0.1; reference Mach number, 0.094.

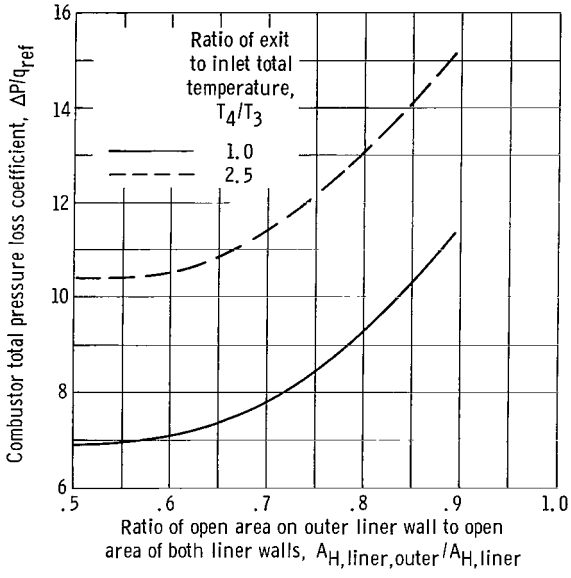

Figure 13. - Effect of increasing fraction of liner total open hole area on outer wall on total pressure loss coefficient. Ratio of liner cross-sectional area to reference area, 0.6; ratio of liner open area to reference area, 0.8; ratio of dome open area to liner open area, 0.1; reference Mach number, 0.094.

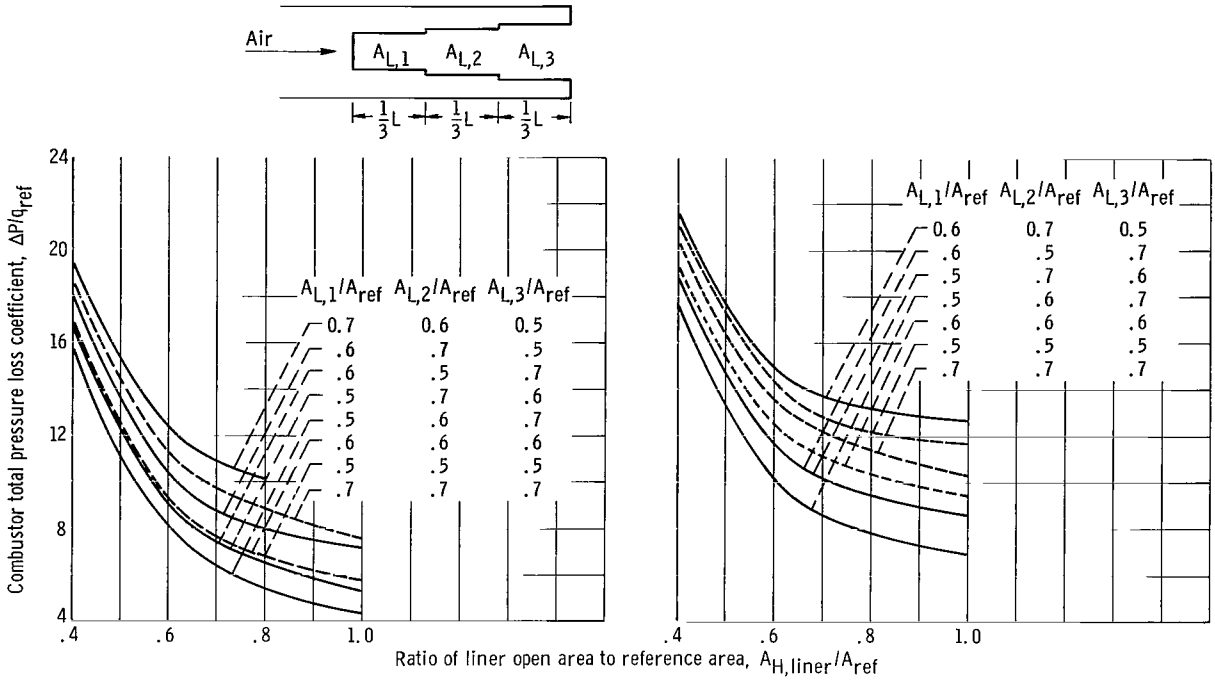

(a) Ratio of exit to inlet total temperature, 1.0.

(b) Ratio of exit to inlet total temperature, 2.5.

Figure 14. - Comparison of effects of constant and varying liner cross-sectional area on total pressure loss coefficient. Ratio of dome open area to liner open area, 0.1; reference Mach number, 0.094.

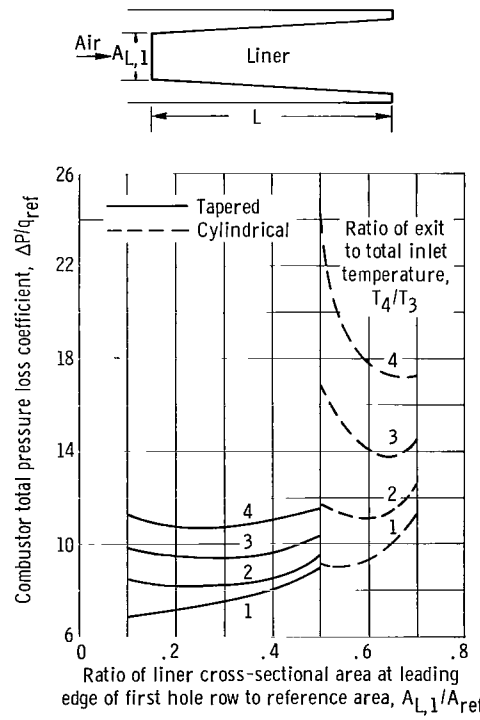

Figure 15. - Comparison of effects of constant liner cross-sectional area and conical liner on total pressure loss coefficient. Ratio of liner open area to reference area, 0.6; ratio of dome open area to liner open area, 0.1; reference Mach number, 0.094.

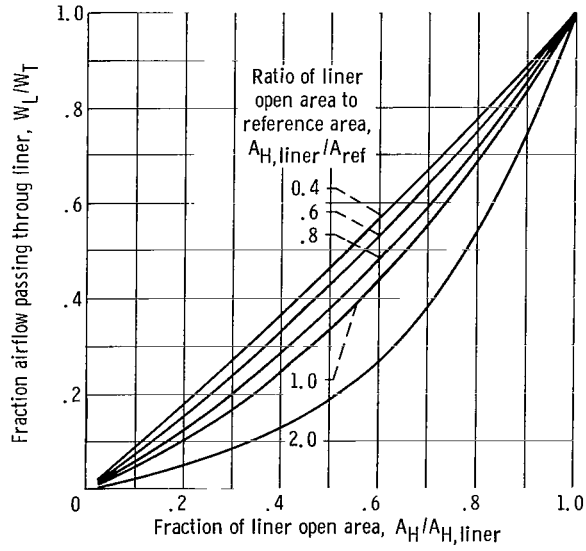

Figure 16. - Effect of liner open hole area on liner airflow distribution with no dome flow. Ratio of liner cross-sectional area to reference area, 0.6; ratio of dome open area to liner open area, 0; ratio of exit to inlet total temperature, 1.0; reference Mach number, 0.063.

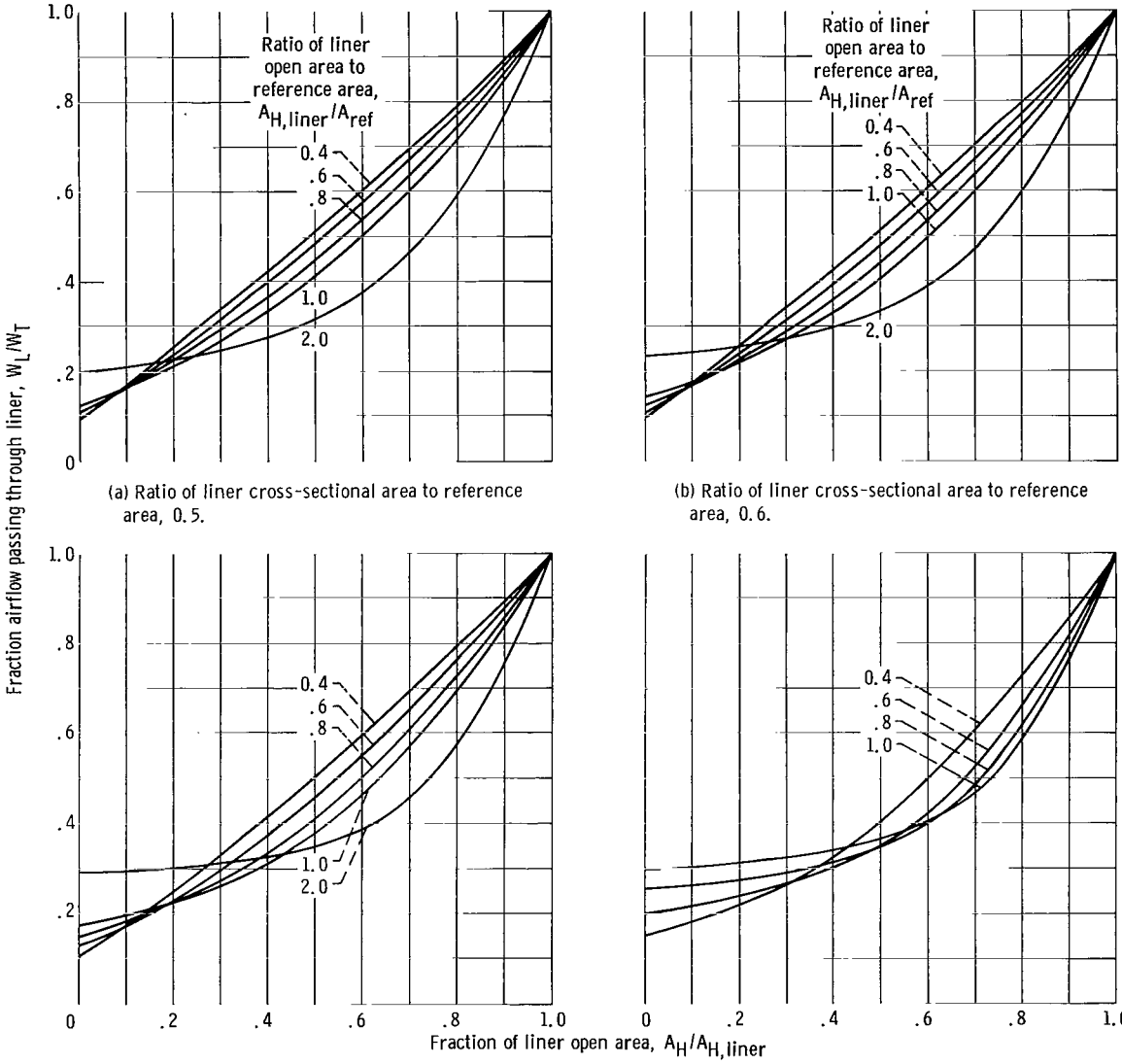

(a) Ratio of liner cross-sectional area to reference area, 0.5.

(b) Ratio of liner cross-sectional area to reference area, 0.6.

(c) Ratio of liner cross-sectional area to reference area, 0.7.

(d) Ratio of liner cross-sectional area to reference area, 0.85.

Figure 17. - Effect of liner open hole area on liner airflow distribution with dome flow. Ratio of dome open area to liner open area, 0.1; ratio of exit to inlet total temperature, 1.0; reference Mach number, 0.063.

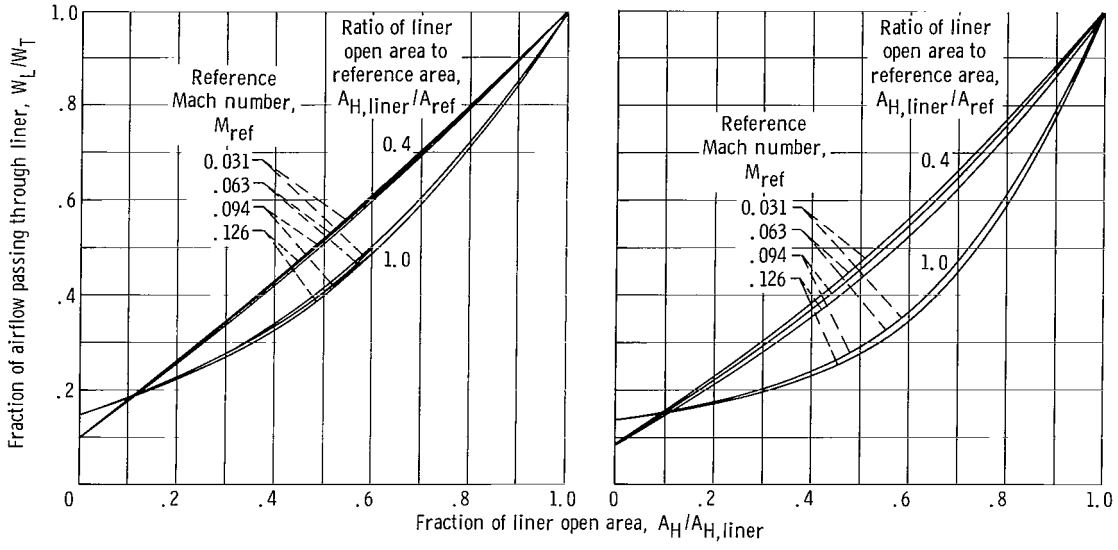

(a) Ratio of exit to inlet total temperature, 1.0.

(b) Ratio of exit to inlet total temperature, 3.0.

Figure 18. - Effect of reference Mach number on liner airflow distribution. Ratio of liner cross-sectional area to reference area, 0.6; ratio of dome open area to liner open area, 0.1.

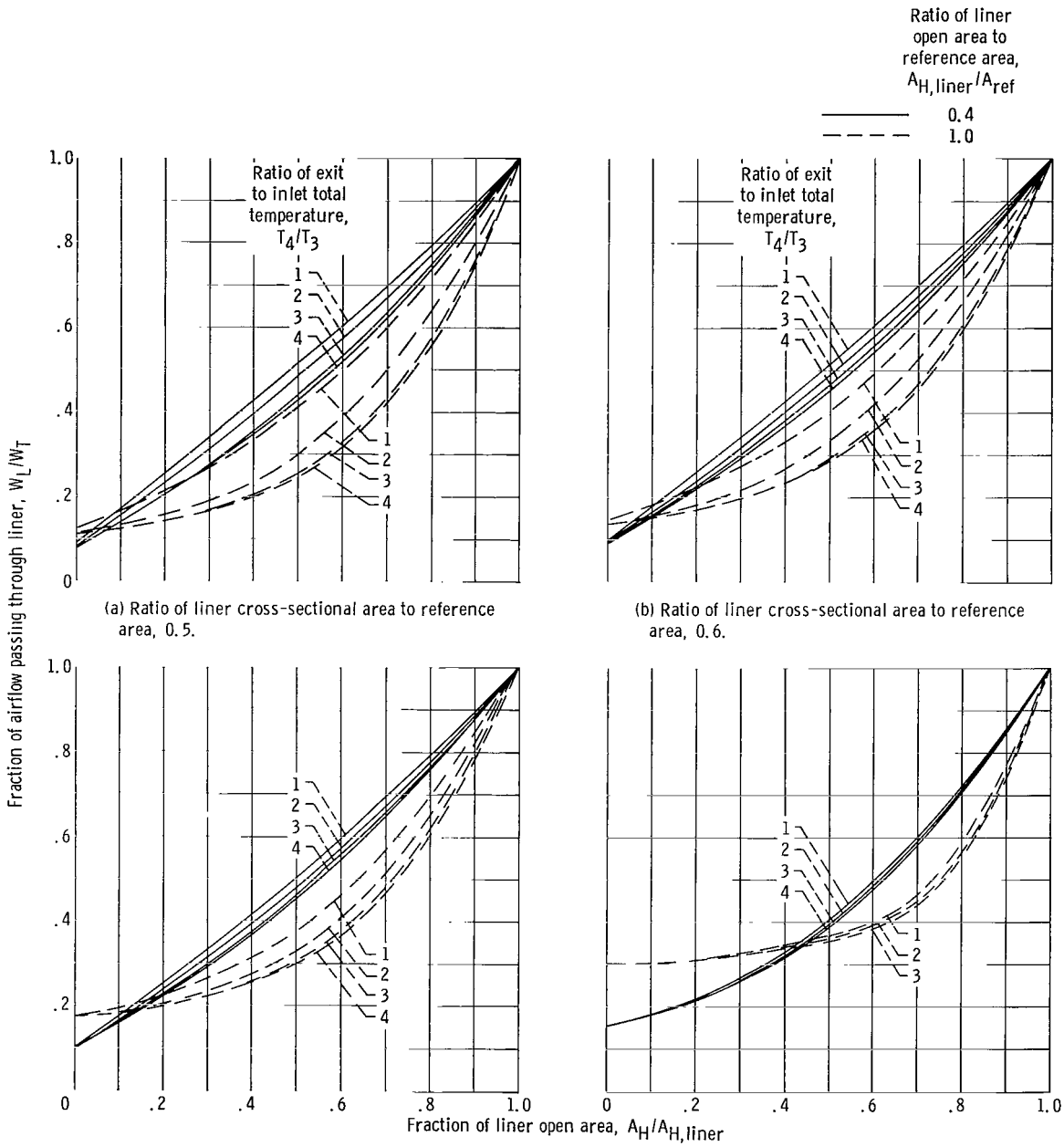

(a) Ratio of liner cross-sectional area to reference area, 0.5.

(b) Ratio of liner cross-sectional area to reference area, 0.6.

(c) Ratio of liner cross-sectional area to reference area, 0.7.

(d) Ratio of liner cross-sectional area to reference area, 0.85.

Figure 19. - Effect of heat release on liner airflow distribution. Ratio of dome open area to liner open area, 0.1; reference Mach number, 0.063.

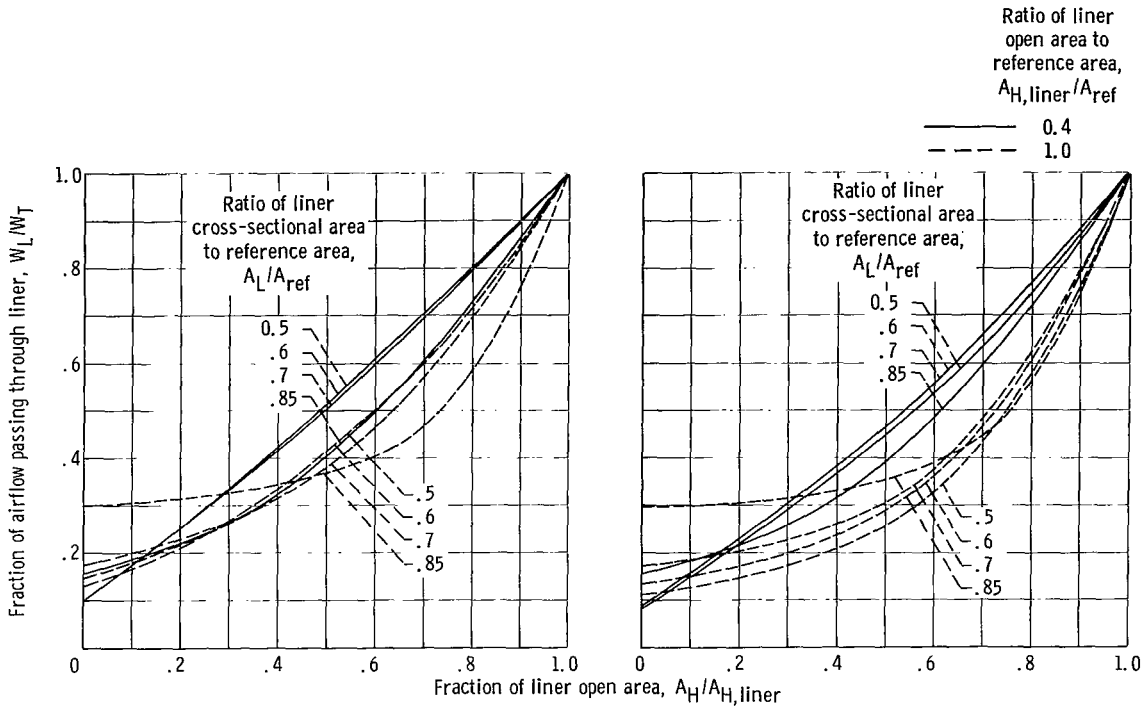

(a) Ratio of exit to inlet total temperature, 1.0.

(b) Ratio of exit to inlet total temperature, 3.0.

Figure 20. - Effect of liner cross-sectional area on liner airflow distribution. Ratio of dome open area to liner open area, 0.1; reference Mach number, 0.063.

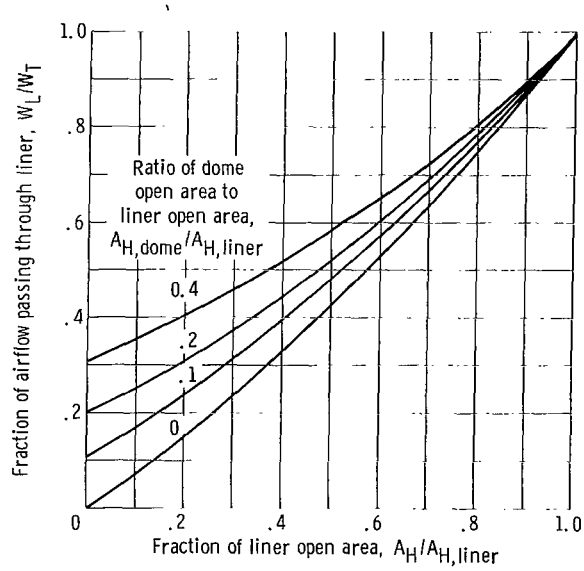

Figure 21. - Effect of open area in dome on liner airflow distribution. Ratio of liner cross-sectional area to reference area, 0.6; ratio of liner open area to reference area, 0.8; ratio of exit to inlet total temperature, 1.0; reference Mach number, 0.063.

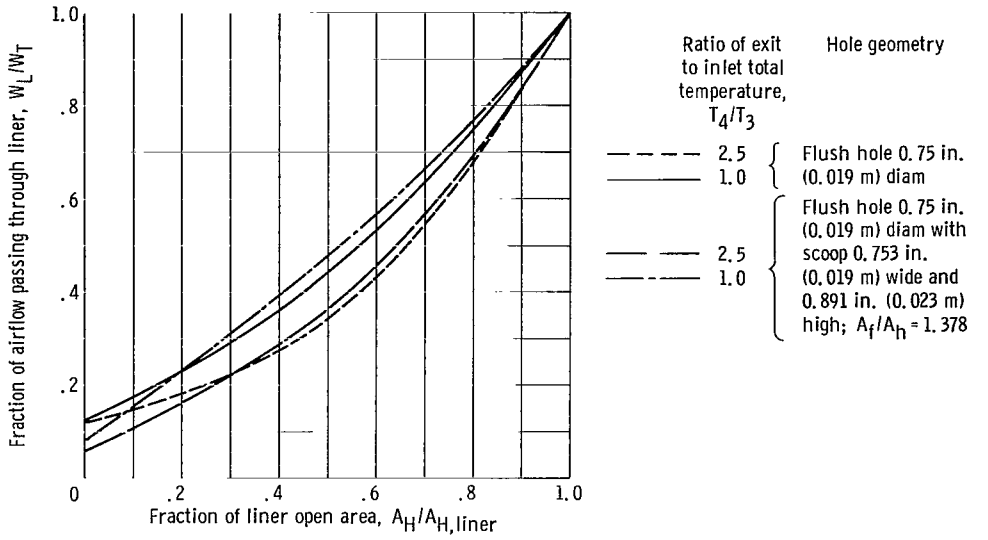

Figure 22. - Effect of liner hole geometry on liner airflow distribution. Ratio of liner cross-sectional area to reference area, 0.6; ratio of dome open area to liner open area, 0.1; ratio of liner open area to reference area, 0.8; reference Mach number, 0.094.

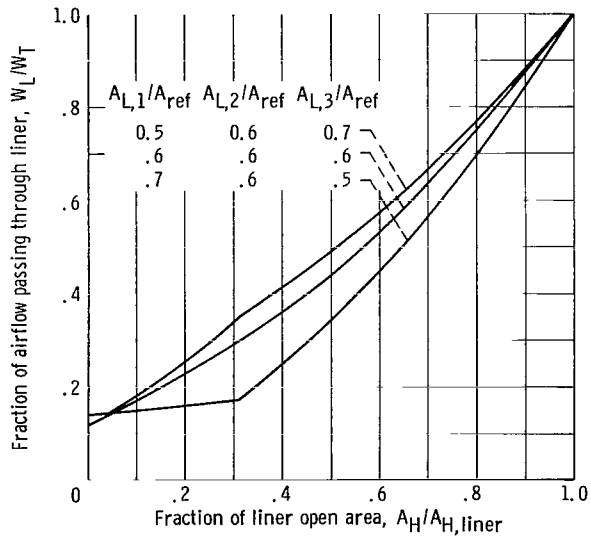

Figure 23. - Comparison of effect of a varying liner cross-sectional area and a constant liner cross-sectional area on liner airflow distribution. Ratio liner open area to reference area, 0.8; ratio of dome open area to liner open area, 0.1; ratio of exit to inlet total temperature, 1.0; reference Mach number, 0.094.

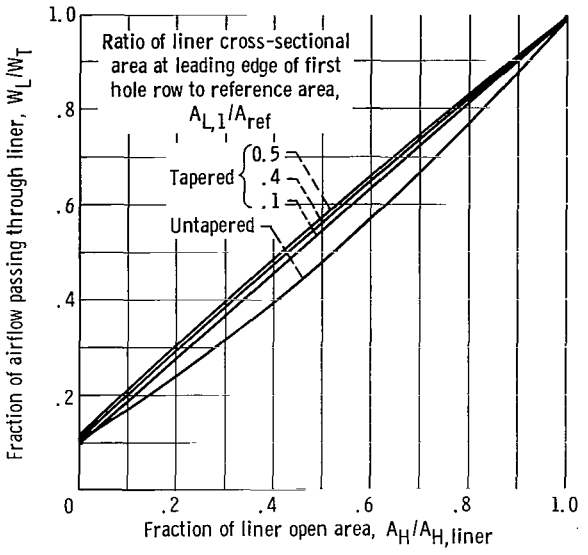

Figure 24. - Comparison of effects of a constant liner cross-sectional area and a conical liner on liner airflow distribution. Ratio of liner open area to reference area, 0.6; ratio of dome open area to liner open area, 0.1; ratio of exit to inlet total temperature, 1.0; reference Mach number, 0.094. Ratio of untapered cylindrical liner cross-sectional area to reference area, 0.6.

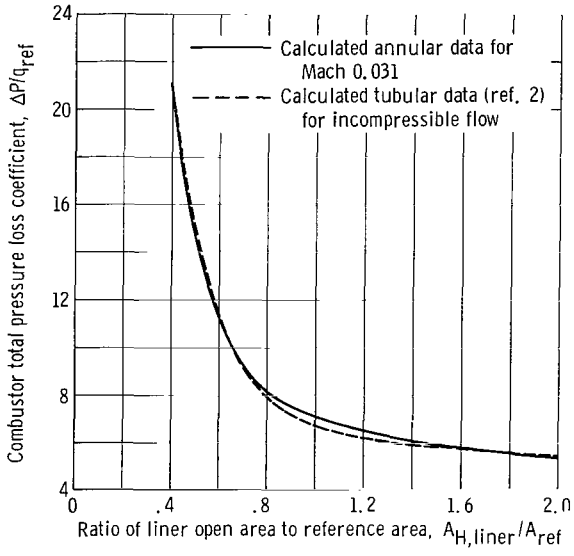

Figure 25. - Comparison of effect of liner open hole area on total pressure loss coefficient for calculated annular and calculated tubular data. Ratio of liner cross-sectional area to reference area, 0.6; ratio of dome open area to liner open area, 0; ratio of exit to inlet total temperature, 1.0.

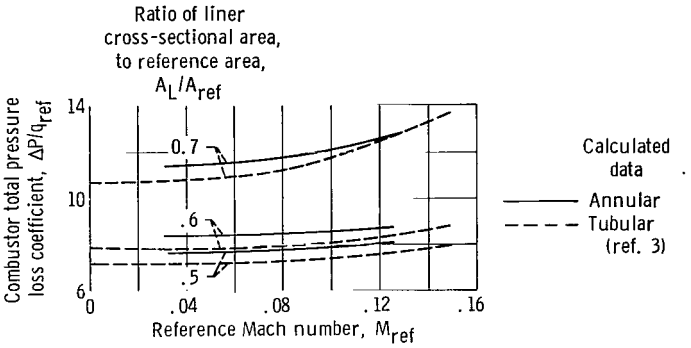

Figure 26. - Comparison of effect of reference Mach number on total pressure loss coefficient for calculated annular and calculated tubular data. Ratio of liner open area to reference area, 0.8; ratio of dome open area to liner open area, 0; ratio of exit to inlet total temperature, 1.0.

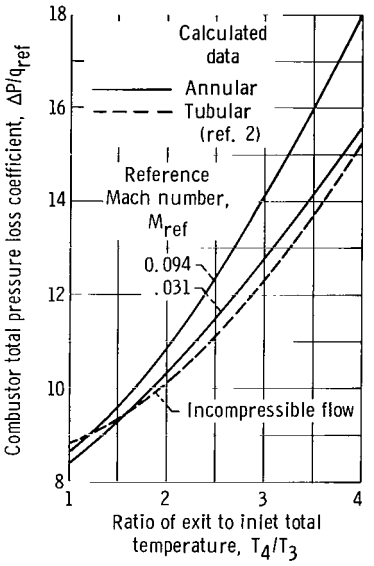

Figure 27. - Comparison of effect of heat release on total pressure loss coefficient for calculated annular and calculated tubular data. Ratio of liner cross-sectional area to reference area, 0.6; ratio of liner open area to reference area, 0.8; ratio of dome open area to liner open area, 0.

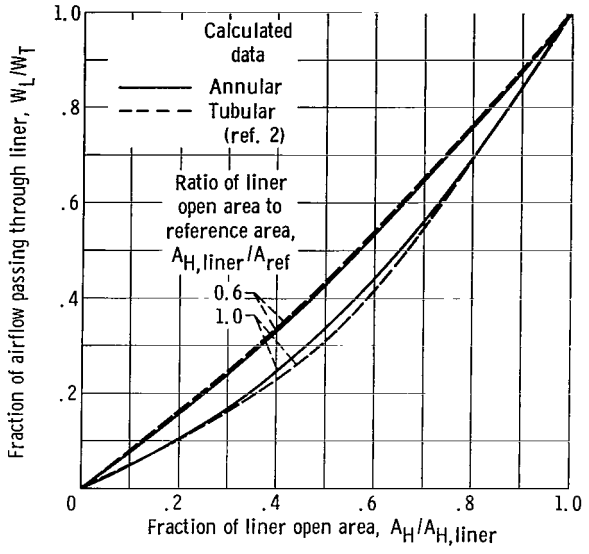

Figure 28. - Comparison of effect of liner open hole area on liner airflow distribution for calculated annular and calculated tubular data. Ratio of liner cross-sectional area to reference area, 0.6; ratio of dome open area to liner open area, 0; ratio of exit to inlet total temperature, 1.0; annular reference Mach number, 0.063; tubular reference Mach number, 0.05.

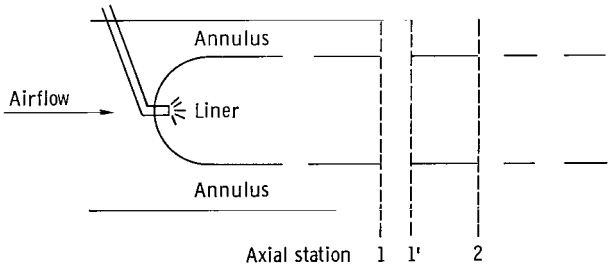

Figure 29. - Air entry ports. (Axial stations are located at front edge of hole rows: 1 refers to current axial station; the prime refers to a station immediately downstream of holes where air is assumed to undergo sudden expansion; 2 is front edge of next hole row.)

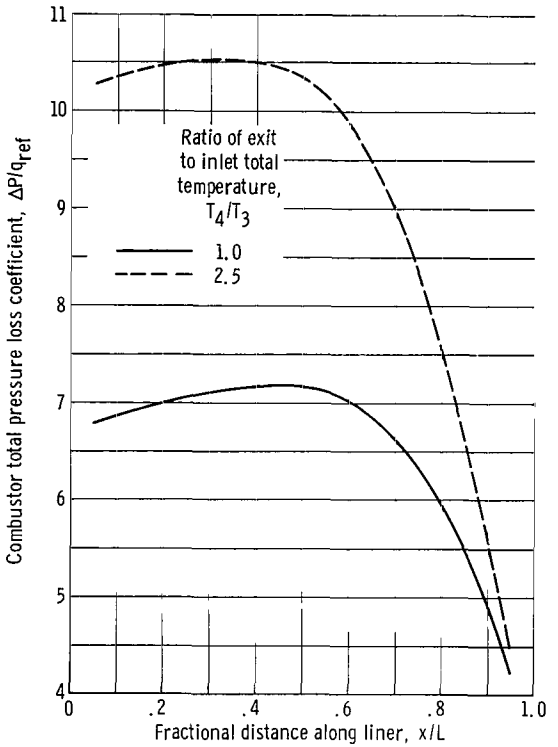

Figure 30. - Effect of defined primary zone length on total pressure loss coefficient. Ratio of liner cross-sectional area to reference area, 0.6; ratio of liner open area to reference area, 0.8; ratio of dome open area to liner open area, 0.1; reference Mach number, 0.094.

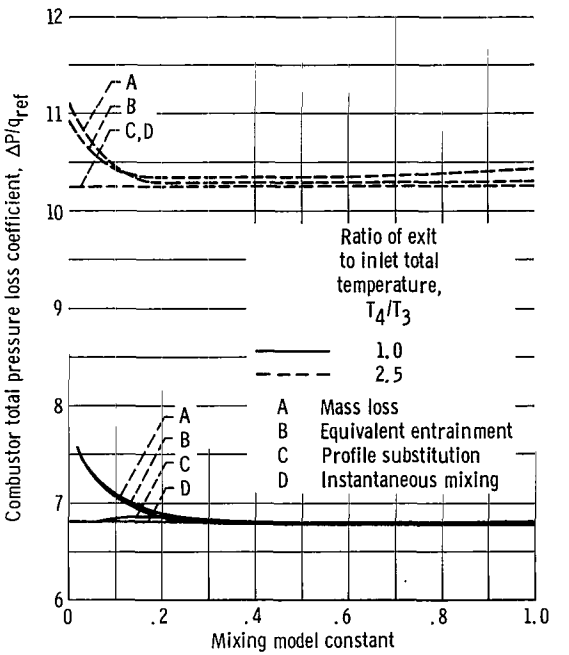

Figure 31. - Effect of mixing model and mixing model constant on total pressure loss coefficient. Ratio of liner cross-sectional area to reference area, 0.6; ratio of liner open area to reference area, 0.8; ratio of dome open area to liner open area, 0.1; reference Mach number, 0.094.

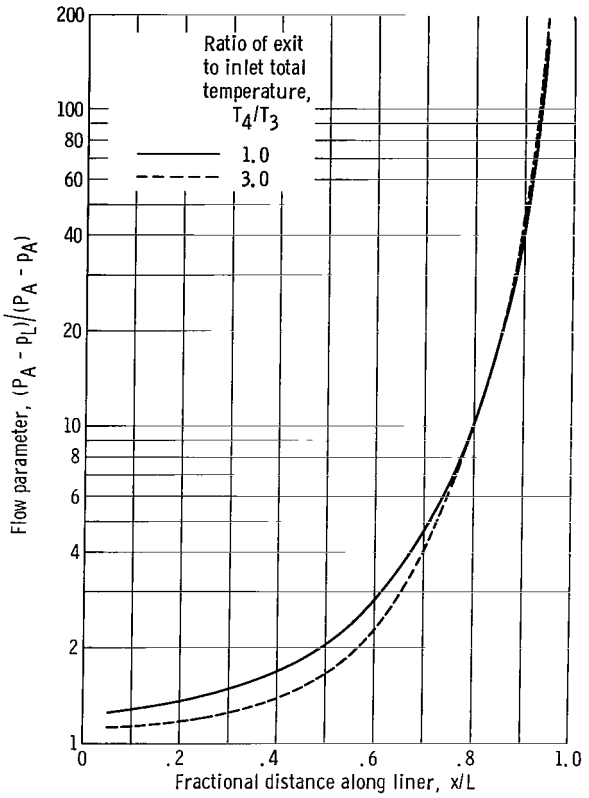

Figure 33. - Variation in flow parameter along combustor. Ratio of liner cross-sectional area to reference area, 0.6; ratio of liner open area to reference area, 1.0; ratio of liner open area to reference area, 0.1; ratio of dome open area to liner open area, 0.1; reference Mach number, 0.094.

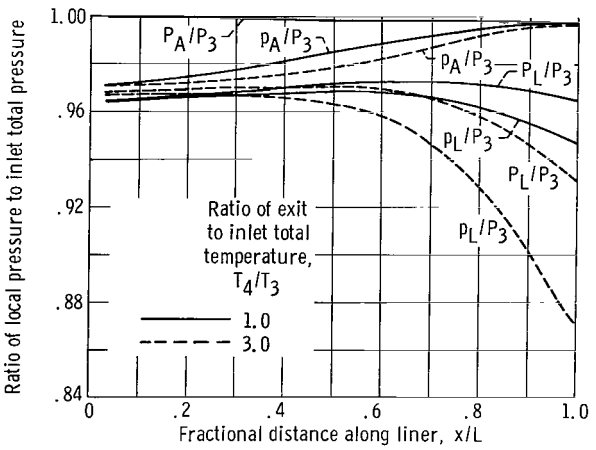

Figure 32. - Variation in total and static pressures in annulus and liner along combustor axis. (Static and total pressures along length of combustor referenced to inlet total pressure.) Ratio of liner cross-sectional area to reference area, 0.6; ratio of liner open area to reference area, 1.0; ratio of dome open area to liner open area, 0.1; reference Mach number, 0.094.

"The aeronautical and space activities of the United States shall be conducted so as to contribute . . . to the expansion of human knowledge of phenomena in the atmosphere and space. The Administration shall provide for the widest practicable and appropriate dissemination of information concerning its activities and the results thereof."

—NATIONAL AERONAUTICS AND SPACE ACT OF 1958

NASA SCIENTIFIC AND TECHNICAL PUBLICATIONS

TECHNICAL REPORTS: Scientific and technical information considered important, complete, and a lasting contribution to existing knowledge.

TECHNICAL NOTES: Information less broad in scope but nevertheless of importance as a contribution to existing knowledge.

TECHNICAL MEMORANDUMS: Information receiving limited distribution because of preliminary data, security classification, or other reasons.

CONTRACTOR REPORTS: Scientific and technical information generated under a NASA contract or grant and considered an important contribution to existing knowledge.

TECHNICAL TRANSLATIONS: Information published in a foreign language considered to merit NASA distribution in English.

SPECIAL PUBLICATIONS: Information derived from or of value to NASA activities. Publications include conference proceedings, monographs, data compilations, handbooks, sourcebooks, and special bibliographies.

TECHNOLOGY UTILIZATION PUBLICATIONS: Information on technology used by NASA that may be of particular interest in commercial and other non-aerospace applications. Publications include Tech Briefs, Technology Utilization Reports and Notes, and Technology Surveys.

Details on the availability of these publications may be obtained from:

SCIENTIFIC AND TECHNICAL INFORMATION DIVISION

NATIONAL AERONAUTICS AND SPACE ADMINISTRATION

Washington, D.C. 20546